CHALMERS
UNIVERSITY OF TECHNOLOGY

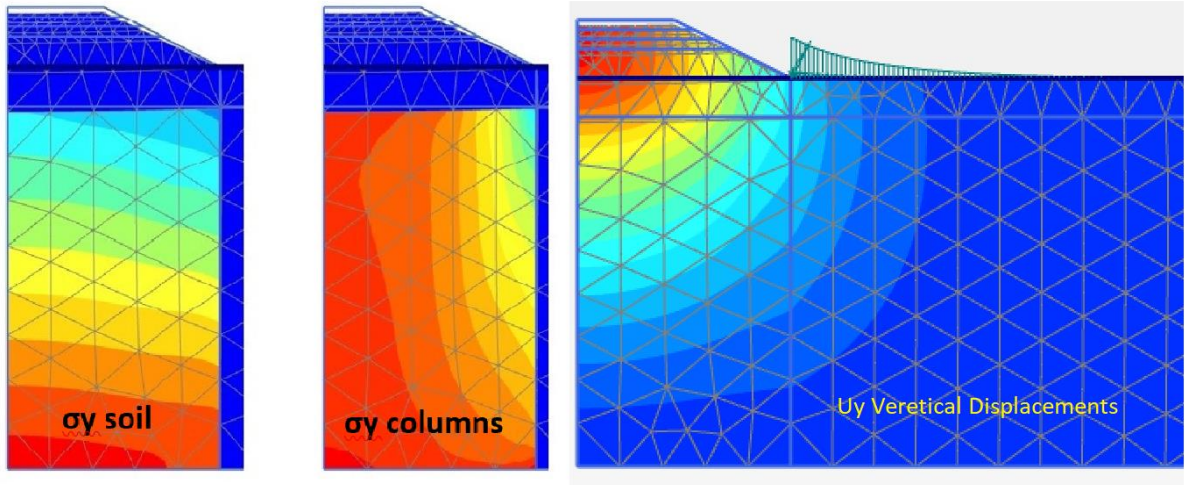

Swedish Method and Volume Averaging Technique in Deep Mixing analysis

A comparison Between Swedish Method and Volume Averaging Techniques using Plaxis 2D

Master Thesis in Infrastructure and Environmental Engineering MPIEE

Sameer Sheikho

DEPARTMENT OF ARCHITECTURE AND CIVIL ENGINEERING

DIVISION OF GEOLOGY AND GEOTECHNICS

CHALMERS UNIVERSITY OF TECHNOLOGY

Gothenburg, Sweden 2024
www.chalmers.se

Master Thesis 2024

Swedish Method and Volume Averaging Technique in Deep Mixing analysis

A comparison Between Swedish Method and Volume Averaging Techniques using Plaxis 2D

Sameer Sheikho

DEPARTMENT OF ARCHITECTURE AND CIVIL ENGINEERING
DIVISION OF GEOLOGY AND GEOTECHNICS

Chalmers University of Technology
Gothenburg Sweden 2024

Abstract

Ground improvement methods are commonly used to improve the stiffness and the settlement of soft soils. Deep mixing method using grouting additives is one of these ground improvement methods. Lime-cement columns ground improvement method is one of the most usable methods in Europe, Asia and Scandinavians countries. In this thesis an embankment constructed on lime-cement and a soft clay soil layer is studied and calculated by tow calculations methods. The manual Swedish method, and the finite element method using volume averaging techniques with Plaxis 2D. The aim of the study is to calculate the deep mixing effects on studied soft soil by using manual Swedish method and volume averaging techniques method with Plaxis 2D, and to compare the results and the main differences, benefits and shortcomings between these tow methods.

Keywords: Deep mix, Lime-Cement Columns, Swedish Method, Volume Averaging Techniques, S-CLAY1S, MNhard, Embankment, Plaxis 2D.

Acknowledgement

I would like to thank my supervisor and Examiner professors at Chalmers University of Technology for giving me the opportunity to take and study this subject, and for their valuable guidance and support. Special thanks to my supervisor Dr Ayman Abed, a senior lecturer at Chalmers University of Technology, without his help the VAT modelling in Plaxis 2D would not been possible.

I would like to express my gratitude towards the whole lecturers and professors who taught me in Chalmers University of Technology, for their valuable information, efforts, and latest updates of engineering knowledge.

Sameer Sheikho, Gothenburg, June 2024

Acronyms

CSV	The combined soil stabilisation with vertical columns
CDM	Cement Deep Mixing
DDM	Dry Deep Mixing (DDM)
DJM	Dry Mixing Jet
DLM	Deep Lime Mixing
DSM	Deep Soil Mixing
LCC	Lime-Cement Columns
MN	Matsuoka-Nakai
S-CLAY1S	Constitutive clay model
VAT	Volume Averaging Technique
UDSM	User Defined Soil Model

List of Figures

List of Tables

Indices

c	Index for columns
s	Index for soil
eq	Index for homogenised material
lim	Index for limits

Roman Letters

α	Absolute rate of destructuation
b	Plastic deviatoric and volumetric strains relative effectiveness in destroying the soil bonding
c	Cohesion
c_u	Undrained soil cohesion
$c_{u,col}$	Columns undrained cohesion
c_{uk}	Undrained cohesion
$c`$	Effective soil cohesion
$c`_{col}$	Effective column cohesion
$c`_k$	Effective cohesion of improved soil
$c`_{k,col}$	Effective column cohesion
$c`_{k,soil}$	Effective unimproved soil cohesion
c/c	Stabilized columns centre to centre spacing
d	Stabilized columns diameter
e_o	Initial void ratio
f_{lcc}	The compression strength of columns
k	Hydraulic conductivity
m	Hyperbolic power of stress strain
n	Diameter ratio for vertical drains
q	Embankment load, external load from embankment
$q_{col,max}$	The maximum designed load of individual column
$p`$	Mean effective stress
$p`_m$	Yield surface size
$p`_{mi}$	Intrinsic yield surface size
$p`_{ref}$	Reference pressure for hyperbolic stress strain modulus
q_{soil}	The soil remained load
r	Column radius
s	Stabilized columns centre to centre spacing
v	Constant related to load distribution in Swedish method
x_0	Initial bonding amount in S-CLAY1S

Capital roman letters

B	Embankment width/surcharge width
C_v	Vertical consolidation coefficient
D	Stiffness matrice
$\dot{D}^c$	Column material stiffness matrice
$\dot{D}^s$	Unimproved soil stiffness matrice
$\dot{D}^{eq}$	Equivalent improved block stiffness matrice
E	Young modulus
E_{col}	Columns young modulus
E_{oed}	Oedometer Young modulus
E_{50}	Confining secant pressure dependent Young modulus
E_{50}^{ref}	Reference Young modulus at reference pressure
E_{ur}	Confining unloading/reloading Young modulus
$E`$	Effective young modulus
G	Shear modulus
G_{ref}	Reference shear modulus
G_{ref}^{ur}	Reference shear modulus for unloading/reloading
G_{ref}^{50}	Reference shear modulus for primary loading
G_{50}	Shear modulus for primary loading
H	Depth of the soil layer = column length in this case study
K_0	Earth pressure coefficient at rest
$K_{c`}$	Earth pressure coefficient
K_h	Horizontal earth pressure coefficient
M_c	Critical state stress ratio
M_0	Normal consolidation stress ratio (stiffness)
M_L	Pre-consolidation stress ratio (stiffness)
M_{soil}	Soil stiffness for unimproved soil
M_{block}	Columns-soil improved block stiffness
L_D	Longest drain path within the columns
OCR	Over consolidation ratio
POP	Pre-overburden pressure

R_f	Failure ratio
S	Settlement
S_{col}	Column settlement
S_{soil}	Soil settlement
S_1^c	Strain matrice distribution between columns and equivalent material
S_1^s	Strain matrice distribution between soil and equivalent material
Z_{lim}	Depth of plastic zone
Z_{block}	Block depth
Zc	Floating zone C depth in Swedish method

Greek letters

α	Columns proportion area per unit m²
α_d	The deviatoric fabric tensor in S-CLAY1S
α_0	Initial yield surface inclination
β	constant related to the column position
β	plastic shear strain and plastic volumetric strain effectiveness ratio
γ_b	Bulk density of soil
γ_{sat}	Saturated density of soil
$\gamma`$	Effective density of soil
γ_w	Water density
γ_s^{ps}	The hardening (plastic part) parameter of objective shear strength
$\dot{\gamma}_{zx}^{eq}$	Plastic shear strain strain in xz plane
δ	Total settlement
δ_A	Plastic zone total settlement in Swedish method
δ_B	Total settlement of zone B in Swedish method
δ_C	Total settlement in floating zone C in Swedish method
ε_{block}	Columns-soil improved block total strain
ε_{col}	Columns total strain
ε_{soil}	Soil total strain
$\dot{\varepsilon}^c$	Total strain increment vector of columns
$\dot{\varepsilon}^s$	Total strain increment vector of unimproved soil

$\dot{\varepsilon}^{eq}$	Total strain increment vector
$\dot{\varepsilon}_y^{eq}$	Total Cartesian strain in y direction
ε_v^p	Plastic volumetric strain
ξ	Absolute rate of destruction
ξ_d	Relative effectiveness rate of destruction
η_{LC}	Load distribution
η	Stress ratio *q/p`*
κ	Swelling line slope index
λ	Compression line slope index
σ_{block}	Columns-soil improved block total stress
σ_d	The deviatoric stress tensor in S-CLAY1S
σ_{soil}	Soil total stress
σ_{col}	Columns total stress
$\dot{\sigma}^{eq}$	Total stress increment vector
$\sigma`$	Effective stress
$\sigma`_c$	Soil pre-consolidation effective stress
$\sigma`_{col}$	Columns effective stress
$\dot{\sigma}`^s$	Effective unimproved soil stress increment vector
$\dot{\sigma}`^c$	Effective unimproved columns stress increment vector
$\sigma`_h$	Horizontal effective stress of the soil
$\sigma`_{v0}$	In-situ soil effective stress
$\sigma`_{ult}$	The strength of the columns effective stress
$\dot{\sigma}_x$	Total stress increment vector on cartesian x direction
$\dot{\sigma}_z$	Total stress increment vector on cartesian z direction
τ_{fdk}	Drained shear strength
τ_{uk}	Undrained shear strength
$\dot{\tau}_{xy}^{eq}$	Shear stress on cartesian xy plane
$\dot{\tau}_{xy}^{eq}$	Shear stress on cartesian xy plane
$\dot{\tau}_{yz}^{eq}$	Shear stress on cartesian yz plane
φ	Total friction angel
$\varphi`$	Effective friction angel

$\varphi`_{k,col}$	Columns effective friction angel
$\varphi`_{m}$	Soil improved friction angel Columns effective friction angel
ψ	Dilatancy
Ω	Volume fraction
Ω_c	Columns volume fraction
Ω_s	Soil volume fraction
ω	Rate of rotation
ω_d	Proportion constant
v	Poisson ratio
$v`$	Effective Poisson ratio
μ	Vertical drains coefficient in Swedish method
μ	Absolute rotation rate of the yield surface in S-CLAY1S

Contents

Table of Contents

1-Introduction

1-1-Background

Soft soils either sand, silt, clay, or a mixture of them were always challenging topics for engineers, the construction process on/or within soft soils in many cases resulted huge and unpredictable problems, which needed to be anticipated in advance and to be solved for making the constructions and the infrastructures usable for human beings. Soil improvement methods are commonly used to enhance soil stabilization and soil mechanical properties. During the evolution of construction and soil mechanic science many soil improvement methods and techniques were invented, grouting injection methods are an important sort of these soil improvement methods and techniques. Stabilization of soft soils is one of the most common problems in geotechnical engineering. “Soil stabilization” refers to any physical, chemical, or biological methods used to improve the engineering properties of a natural soil to make it serve adequately an intended engineering purpose.(Hossain et al, 2006). Grouting injection methods has been widely used to improve both stabilization and stiffness of soft soils especially soft clay, which shows significant changes in stiffness and stability if the water content and the hydrology conditions are changed. (Toll et al., 2012). Grouting injection methods using lime-cement mixture was developed in 1970 in Japan and Sweden. The improvement of soft clay ground using Lime-cement can be done by two techniques:

The first one is using dry jet mixing (DJM) which delivers a dry powder of lime, cement, or both mix of them into the ground making a mix of soil-cement, soil-lime, or soil cement-lime columns. This method first reported to be successful in 1980. It is widely used in Europe and Nordic countries and later in USA and Asia (Hossain et al, 2006). The second technique” chemico-pile” includes casting of treated lime in the soil without mixing with the soil. This method is used in Japan and Singapore. There is another method called wet mix which uses a wet mixture of lime or cement in slurry form instead of dry powder. The Deep mixing is used in Sweden since 1970, it provides more economical benefits if compared to the other soil improvement methods. (Larsson, 2006) Life cycle analysis of soil improvement methods shows using binder stabilizers are much advantageous in saving energy and transport consumptions. Deep mixing soil improving method can be used as an environmentally friend with low CO_2 emissions and cost effective alternative of piling methods (Becker, Karstunen, 2013). Dry Deep Mixing (DDM) is currently accepted worldwide as ground improvement method. (Larsson, 2021). Where binders, often cement and lime, are mixed with soil by using rotating mixing tools figure (1). The resulted improved soil has much higher stiffness and deformation resistance properties. Mass stabilization method is often used with peat or mud soils due to their weakness and volumetric changes (Larsson, 2021).

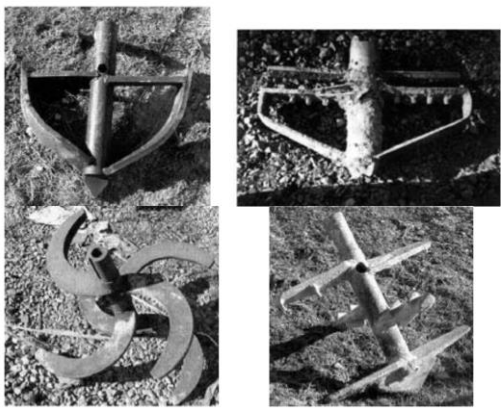

Figure 1 Horizontal blades at the tip of the mixing tool.(Kempfert, 2006)

1-2-Aim

The aim of this thesis is to investigate the Swedish method for designing deep mixing soil improvement in terms of settlement and stability of an embankment on soft clay with lime-cement columns and compare it with Volume Averaging method using finite element Plaxis 2D software. To try to analyse the following questions:

- How do the settlements calculated by the Swedish method compared to the settlements obtained from Volume Averaging Techniques using Finite element analysis with Plaxis 2D
- How do the differences in results validate the theoretical estimations of both calculation methods.

1-3-Limitations

There are several limitations in this thesis, furthermore, each used method had its affected limitation on the performed work and results.

- The studied improved soil is layered above a firm soil layer, no floating columns and this simplifies the hand calculations, which were calculated by Excel.
- The model for Swedish method calculations consists only of one soft soil layer.
- The simple mathematical equation of Swedish method simplifies the consolidation behaviour of the improved soil, which is not always a correct approach.
- The theoretical estimation of horizontally layered soil does not always exist in situ conditions for Swedish method calculations.
- The multi soil layers has its impact on Swedish method as it doesn't predict the location or the depth of plastic layer.
- There are no laboratory tests to compare the estimated improved column parameters with.
- There are no in situ observations for the estimated typical soil model, which is estimated in this thesis to compare theoretical results with field observations.

1-4-Method overview

The methodology was divided into five main steps: literature study of soil improvement using Swedish method, literature study of Eurocode 7 based on Vogler 2008. literature study of soil improvement using Volume Averaging Techniques, Swedish method hand or Excel calculations, and calculations results of Volume Averaging method using finite element Plaxis 2D software. The literature study was performed to describe soil improvement methods in general, and to describe the principals of Swedish method, serviceability limit state according to the Eurocode, and Volume Averaging method using Plaxis 2D software. Swedish method and Eurocode method for calculating settlements were performed by Excel, which helped a lot to change parameters easily and made comparisons between the estimated columns diameters and spacings. The final result charts were made by Excel as well.

S-Clay1S and MN-hard model were used to model soil and lime-cement columns in numerical finite element modelling software Plaxis. The focus on this thesis was on isotropic conditions and thus any effect of anisotropy was left out.

2-Theory

2-1-Deep Mixing

2-1-1-Dry Deep Mixing

Dry deep mixing methods were developed in Sweden and Japan almost parallel since 1960s. (Kempfert, 2006). At earliest phases of method development lime was used as binders, later a defined cement amounts were added to the lime as mixed binders. Stiffer and stronger material can be produced by mixing a defined ratio of lime and cement with soft soils. This procedure reduces settlements dramatically because of the new stiffer emerged material, and increases the safety against failure due to its comparatively high compression strength (Alén et al., 2005a). The obtained shear strength is higher from 10 to 50 times than the shear strength of natural undistributed soil (Kempfert, 2006). The binders in this method are mixed with soil in powder form, as a mixture of unslaked lime and cement, gypsum, pulverised fuel ash, or slag can be added or used as binders.(Vogler, 2008)

2-1-2-Wet Deep Mixing

Wet deep soil mixing uses in-situ mixture of cement or lime-cement mix in slurry form injected to the soil, the advantage of this method is that it can be applied to a depth of 50m. Where the slurry injects to the soil through hollow rotating mixing shaft with various types of cutting tools at its tip. (Kempfert, 2006). The most common binder is cement in this mixing method, plus various additives can be added (EN14679-2005). Table (1) shows the classification of deep mixing methods.

Binder	Condition	How to feed	Method
Lime	Dry	Screw feeding (mechanical)	DLM - Deep Lime Mixing Method
		Compressed air (pneumatic)	DJM – Dry Jet Mixing Method
Cement			Nordic method (Europe)
			DJM – Dry Jet Mixing Method
	Wet	Pumping (liquid feeding)	CDM – Cement Deep Mixing
			European method – Flight auger type

Table 1 Classification of Deep Mixing Methods (Kempfert, 2006)

Figure 2 Typical wet mixing tools. (Topolnicki, 2003)

2-1-3-Chemical Reactions

When adding lime to a clay soil lime or Calcium oxide reacts with the water in clay or silty soils according to this chemical equation:

$CaO + H_2O \rightarrow Ca(OH)_2 + 15.6$ kcal/mol; 280kcal/kg (Hossain et al, 2006).

Filling the voids in soil with chemicals. The calcium hydroxide $Ca(OH)_2$ dissociates into water, increasing PH and the electrolytic concentration of pore water, dissolving AL_2O_3 and SiO_2 from clay particles according to the chemical equation:

$Ca(OH)_2 \rightarrow Ca^{++} + 2(OH)^-$

The dissociation results an ion exchange, flocculation, and a pozzolanic reaction. When adding lime to a clay soil sodium or other cations on the clay's mineral surface exchanges with calcium, this change affects the structural component of the clay minerals. Within minutes to few hours the calcium hydroxide transforms again by the presence of carbonic acid, which is produced in the soil from the reaction of carbon dioxide with soil water. The **dissociation** reaction of lime into Ca^{++} and $(OH)^-$ modifies the electrical surface forces of clay minerals (Hossain et al, 2006).

Ca^{++} + clay → Ca^{++} exchange with monovalent ions (K^+**,** Na^+). As a result, clay particles bonds with each other increasing the shear strength. The shear strength increases with time due to the **pozzolanic** reactions. Where calcium ions Ca^{++} continue to react with AL_2O_3 and SiO_2 in clay and form $Ca.SiO_2.H_2O$ complex causing the improvement of the clay (Hossain et al, 2006).

$Ca^{++} + 2(OH)^- + SiO_2 \rightarrow CSH$

$Ca^{++} + 2(OH)^- + SiO_2 + AL_2O_3 \rightarrow CSH$

The gel of calcium silicates, lime silicates, or both cements and bonds the clay soil particles. The lime or lime-cement columns have considerable strength and they act to reinforce the soil as well as to alter and change its nature (Hossain et al, 2006). Adding lime, cement or lime-cement mix to the soil creates a strong bond that fills the voids in the soil with chemical reaction products (Vogler, 2008), reduces soil water content, and increases the strength and the stiffness of the soil.(Alén et al., 2005a) The reaction continues and progress over time to reach the final stiffness of the lime-cement/soil compound, this final stiffness not only depends on time but also it depends on the ratio of lime-cement amounts which are powdered into the soil. A binder of dry powder will be pumped into the ground with compressed air. In Japan they use a slurry form of the binders in a shape of wet mixing method (Vogler, 2008), as shown in figure (2).

2-1-4-The Applications

Deep mix soil improvement methods are essentially used to increase the strength and the stiffness of soft soils, and to reduce the vertical and horizontal deformations resulted from disturbing the rest conditions of the soft soils by new constructions on/or within the natural soil blocks. In addition of improving soil stiffness and reducing settlements deep mixing applications can used to: include the reduction of soil vibrations caused by traffic movements and neighbouring construction activities, isolation of contaminated soils, increase the bottom stability of deep excavations, stabilisation and strengthening of soils around tunnel borings, active earth pressure reduction, stabilisation of dredged materials, and as a foundation for small buildings (Alén et al., 2005a). As shown in figure (3).

Deep mix soil improvement methods can be considered practically and economically preferable when the following circumstances had existed:

The soil was soft, a constant and continuous supply of binders were applied, treated ground strength was closely engineered and determined, the vertical overhead clearance were relatively unrestricted, and there was no obstructions to the depths of about 30m (Vogler, 2008).

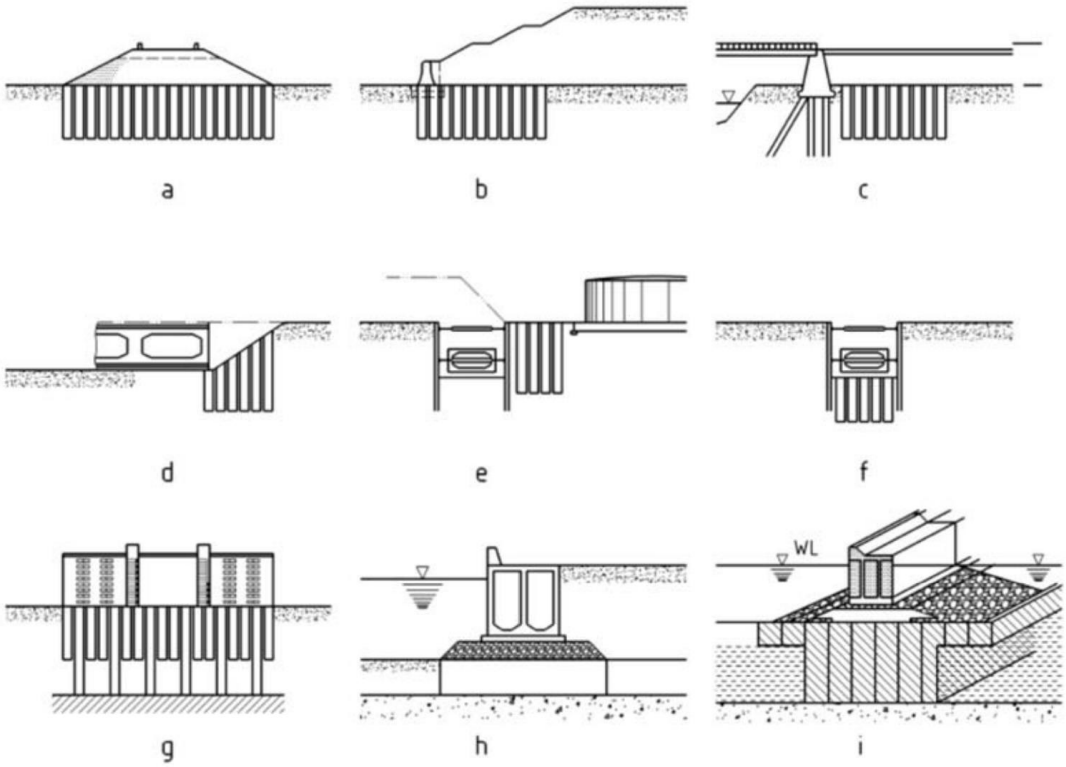

Figure 3 Applications of deep mixing method: a) road embankment; b) fill; c) bridge abutment; d) cut slope; e) nearby constructions; f) braced excavation; g) pile foundation; h) sea wall; i) break water (EN 14679, 2005).

2-1-5-Binders

There are many binders that can be used in deep mixing methods, these binders can be: Quick lime (unslaked lime), cement, lime-cement mixture, gypsum, blast, furnace slag, fly ash, and any other waste material. These binders can be dry mixed with the soil (DJM, or DSM) methods, which are used in Scandinavia region, or wet mixed method which is used in US and Japan (Vogler 2008). Table 2 shows the binder types depending on soil types.

Soil type	Suitable binder
Clay	Lime or lime/cement
Quick clay	Lime or lime/cement
Organic clay and gyttja	Lime/cement or cement/granulated blast furnace slag or lime/gypsum
Peat	Cement or cement/granulated blast furnace slag or lime/gypsum/cement
Sulphate soil	Cement or cement/granulated blast furnace slag
Silt	Lime/cement or cement

Table 2 Binders Commonly Used in Dry Mixing(EN 14679, 2005).

In dry mixing method binders are added to the soil in powder form, they are normally a mixture of lime and cement. There are some other additives that can be added. In wet mixing cement is used in most cases as a binder. The amount and ratios of binders varies according to the soil characteristics and the

mechanical properties, in clays a mixture of lime and cement can give best results of soil improvement (Vogler 2008). Table (3).

Soil type	*Binder*	*Amount of binder*	*Commentary*
Clay	Lime, Cement, Lime/ Cement, Lime/ Cement/Fly Ash	70–110 kg/m³ *Pure cement 90–150 kg/m³*	
Quick clay	Lime, Lime/Cement, Lime/Cement/ Fly Ash	70–100 kg/m³	Quick reaction, especially with high lime content.
Silty clay	Lime/Cement, Cement, Cement/ Slag	70–110 kg/m³	High degree of cementation with cement.
Organic clay	Cement, Lime/ Cement, Cement/ Slag	100–200 kg/m³	Slow reaction, minor part with lime commonly speeds up the reaction.
Sludge	Cement, Cement/Slag	120–250 kg/m³	Slow reaction. Difficult to predict strength increase.
Clay with high sulphide content	Cement, Lime/ Cement, Cement/ Slag	120–250 kg/m³	Slow reaction. Large variations in strength gain. Local knowledge important.
Silt	Cement, Cement/ Slag, Lime/Cement	100–150 kg/m³	
Sandy silt	Cement, Cement/Slag	60–110 kg/m³	Natural moisture content needs to be larger than 30%.
Peat	Cement, Slag/Cement	150–>300 kg/m³	Very important with field and laboratory tests.
Dredged material (Mud)	Cement, Cement/ Slag, Cement/Fly Ash	70–110 kg/m³	Tests necessary, especially due to contaminations.
Contaminated soils		70–110 kg/m³	Tests necessary, especially due to type of contamination and leakage tests.

Table 3 Soil Types and Binders (Kirsch et al, 2012).

In a very high content of organic soils, cement is preferable and can achieve best results. Gypsum and ashes are waste materials, and they are cheap materials, besides they have pozzolanic reactions with certain types of soil. As a precondition of using binders as soil improvement materials laboratory tests must be performed to determine the type and the ratio of binder that can achieve best results for soil improvement. Adding binders to clay soils will increase the bulk density and reduce soil water content generating heat from the reactions between soil particles and water with the binder mix particles. (Åhnberg et al., 2006).

As a result and a conclusion, site-specific requirements, soil characteristics, laboratory results of mixing tests, and local experience are important parts in determining the sufficient type and amount of binders to be mixed with soil (Kirsch et al, 2012).

2-2-Design of Deep Mixing

Increasing the shear strength and/or reducing the settlement (compressibility) are the main objectives of deep mixing soil improvement methods, by mixing soil with chemical additives that react with soil making soil particles bonding, and/or filling soil voids by chemical reaction with the additives (EN 14679, 2005). Figure (4) shows the iterative design process of deep mixing methods.

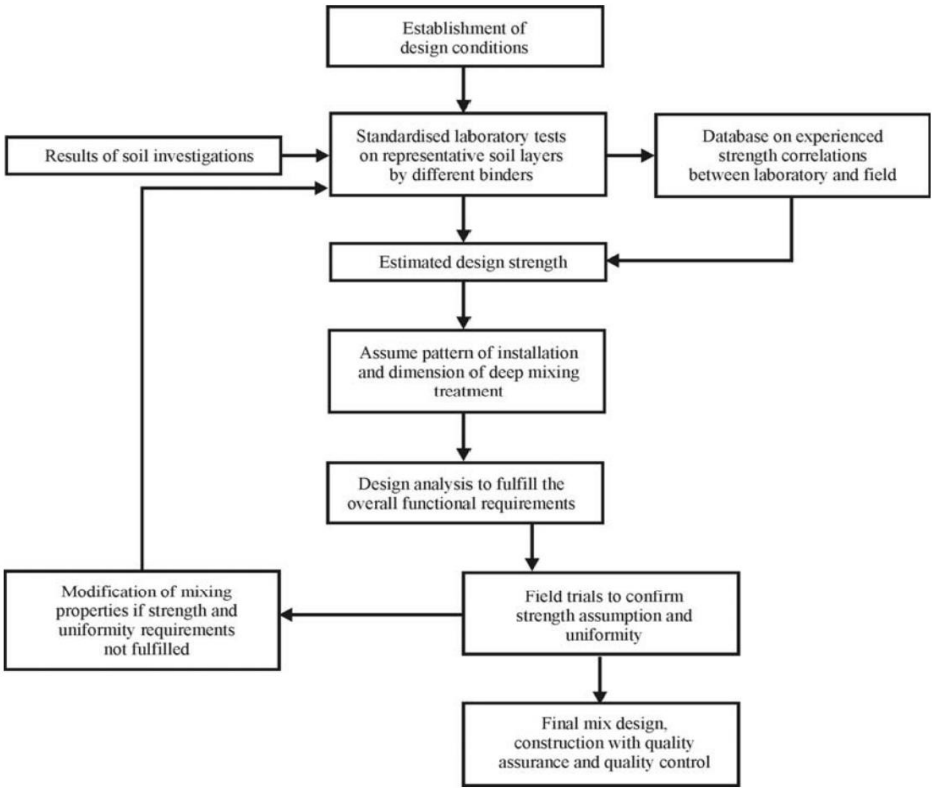

Figure 4 Iterative design process (EN 14679, 2005).

2-2-1-Patterns of Installations

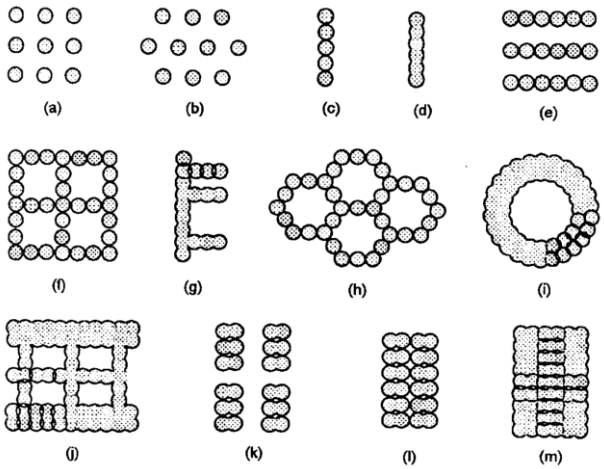

Figure 5 Patterns of Deep Mixing columns. a), b) column type (square and triangular a), b) column type (square and triangular grid), c) tangent column wall, d) secant column wall, e) parallel tangent walls, f) tangent walls with a grid system, g) tangent column wall with buttresses, h) circular cells with tangent columns, i) column groups in a ring form, j) lattice type of group of columns, k) group of secant columns, l), m) block made up of secant columns. (Topolnicki, 2003).

A different patterns of column installations for deep mixing method were developed depending on the purpose of deep mixing. If reducing the settlement was the main purpose an equilateral triangular or square pattern of columns is suitable to be installed, as shown in figure (5). For stability of embankments the columns are installed in walls perpendicular to the expected failure surface (EN 14679, 2005). If the columns are installed for containment purposes, block type, grid type, and wall type is used and they will be putted in overlapping shape.

Figure 6 Column installation (Alén et al., 2005a).

Figure 7 Interlocking Columns in Panels. Upsala, Sweden (Kirsch et al, 2012)

Field equipment for installing deep mix lime-cement columns is usually mounted on large scale. Cement and lime is stored in huge tanks hooked up directly to the machine, there are many different mixing tools for penetrating the soil, in Sweden and most of Europe countries they are all with a diameter of 60 to 80 cm of columns (Alén et al., 2005a). Figure (6) shows the column installation machine. Figure (7) shows a panel interlocking example of columns casting. Figure (8) shows an example of the mixing tool machine and shape. Figure (9) shows some other mixing tools. Mixed column can be used to support a sheet pile retaining structure figure (11). Injected columns can continue to and rest on firm soil layer or can be situated as floating columns, figure (10), in this case the effect of the floating column on the beneath soil layer must be calculated.

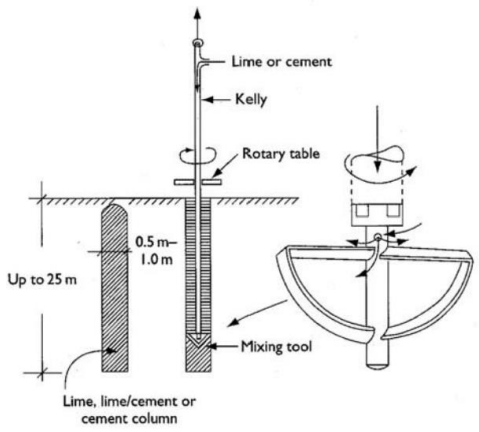

Figure 8 vertical mixing tool (Alén et al., 2005a)

Figure 9 Principle sketch of the traditional mixing tool with semi-circular stirrup and tapered blades and some other examples of mixing tools (Larsson, 2006)

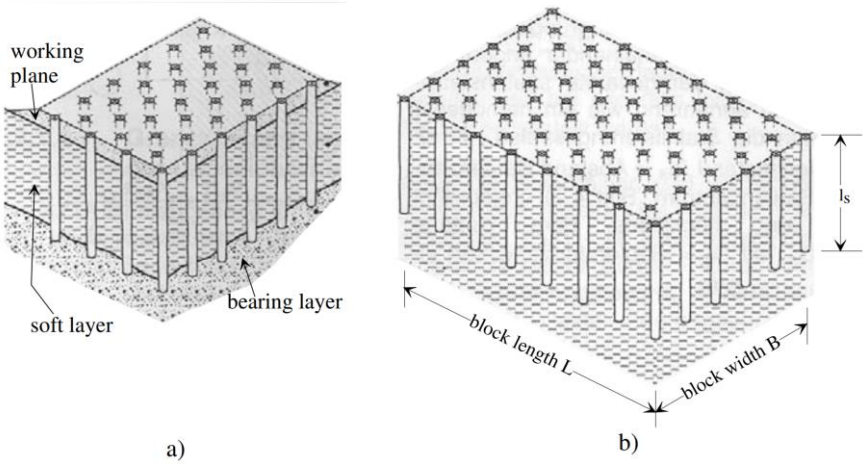

Figure 10 a) CSV-Columns resting on bearing layer, b) Floating CSV-Columns acting as a block (Kempfert, 2006).

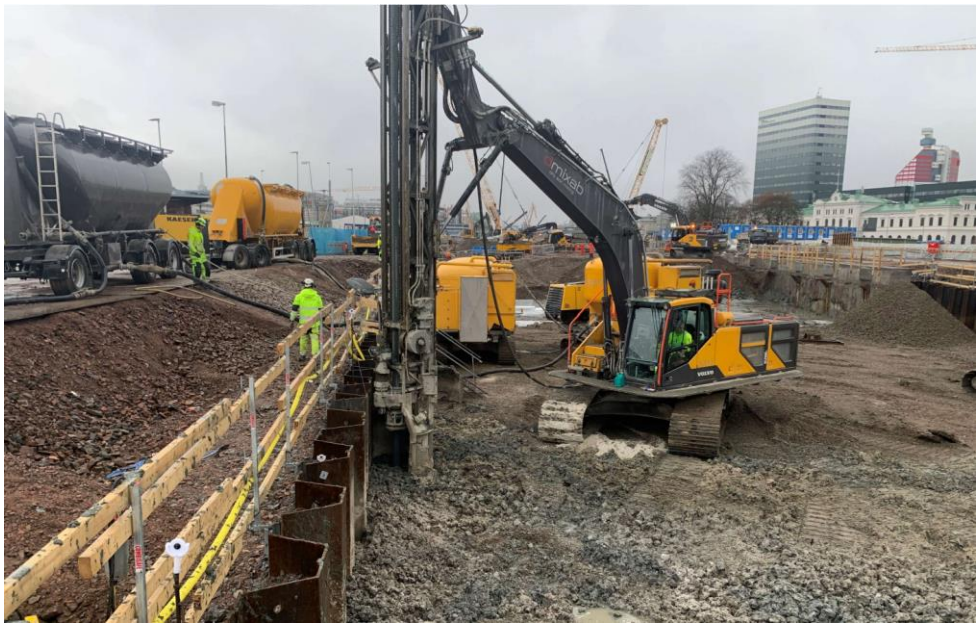

Figure 11 Machine used in Nordic Countries (Larsson, 2021)

2-2-2-Prediction of strength gain

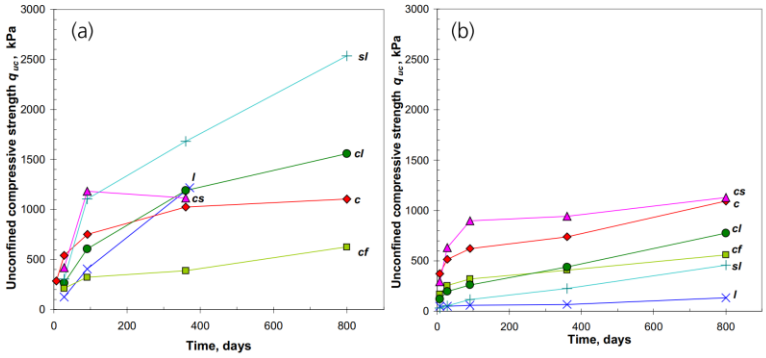

Figure 12 Examples of Measured Strength per Time for Clay with Various Composite Binders (50:50) ratio. C: cement, l:lime, s:slag, f:fly ash. (a) Löftabro clay. (b) Linkoping clay. Quantity of binders 100 kg/m³ (Åhnberg et al., 2006).

The strength gaining per time and the prediction of strength increase according to soil conditions and binder types were investigated by many researchers. Åhenberg (2006) had investigated in clay samples tested from 7 to 800 days. As shown in figure (12) the unconfined compression strength increased with time for most types of binders. For cement stabilised clay the strength prediction can be estimated from the equation B1:

$$\frac{q_t}{q_{28}} = 0.3 \times ln\, t \quad \text{.....B 1(Kirsch et al, 2012)}$$

Where q_t = UCS after t days.

q_{28} = UCS after *28* days

t = time in days.

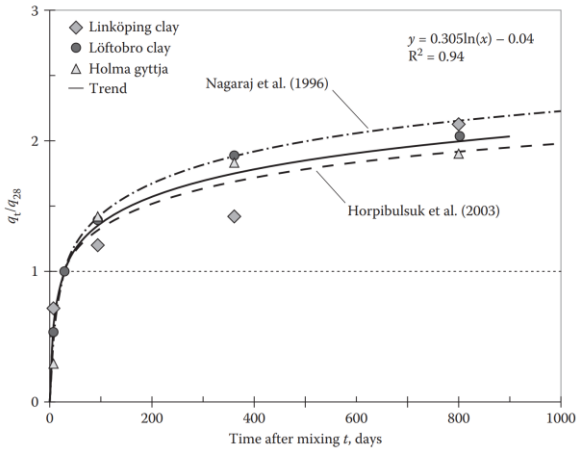

Figure 13 Increase in Unconfined compression strength over time for Cement Stabilised clay (Åhnberg et al., 2006), (Nagaraj et al., 1998), (Horpibulsuk et al., 2003)

3- Design following the Swedish Method

The Swedish method for deep mixing normally divides the soil layer to three zones (Alén et al., 2005a). Figure (14).

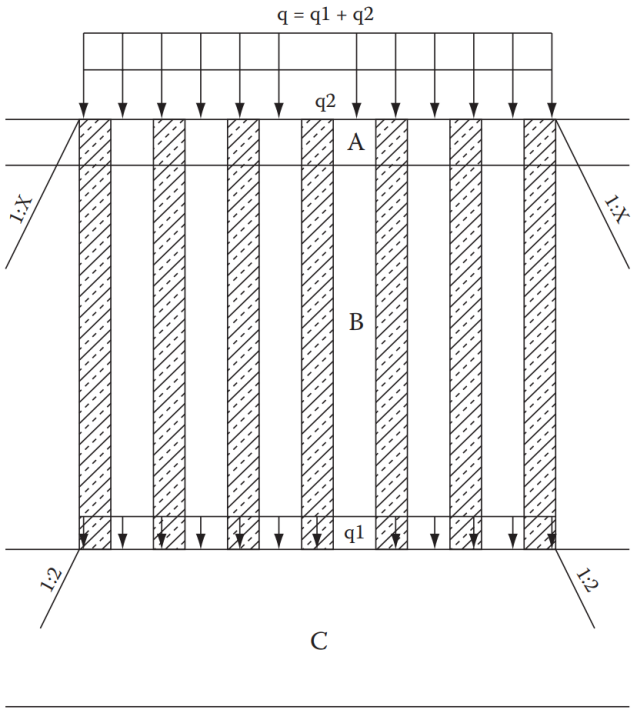

Figure 14 Conceptual Zones. Principle of load split and Stress Distribution from Stabilised Soil Volume (Kirsch et al, 2012)

Zone **A** the upper transition zone, where the columns are fully plastic. Zone **B** the main zone, of composite materials, which considered as an elastic zone. The material properties are given by the weighted mean value of the columns and the soil for the composite material block which includes LCC columns and soil the composite modulus (Alén et al., 2005b). M_{Block} equals:

$$M_{Block} = \alpha . E_{col} + (1 - \alpha) . M_{soil}$$ .....B 2 (Alén et al., 2005a).

Where α is the proportion of columns area per unit area m², $E_{col} = 20 . c_{u,col}^{1.6}$ *or* $E_{col} = 32 . \left(\frac{c_{u,col}^{1.6}}{100}\right)$ is the column module, or it can be defined from lab tests and equals between 20-30 MPa, and M_{soil} the soil modulus can be obtained from soil lab tests. $C_{u,col}$ is the undrained shear strength of the columns and it is restricted to 100 Kpa

$$\alpha = \pi d^2/(4 . s)$$ .....B 3

s is the estimated column spacing c/c (m).

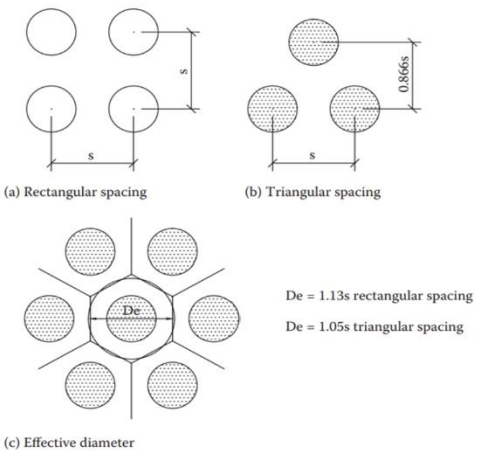

$\alpha = \pi . d^2/4 . s^2$ for rectangular spacing

Figure 15 Ratio of improvement (Kirsch et al, 2012)

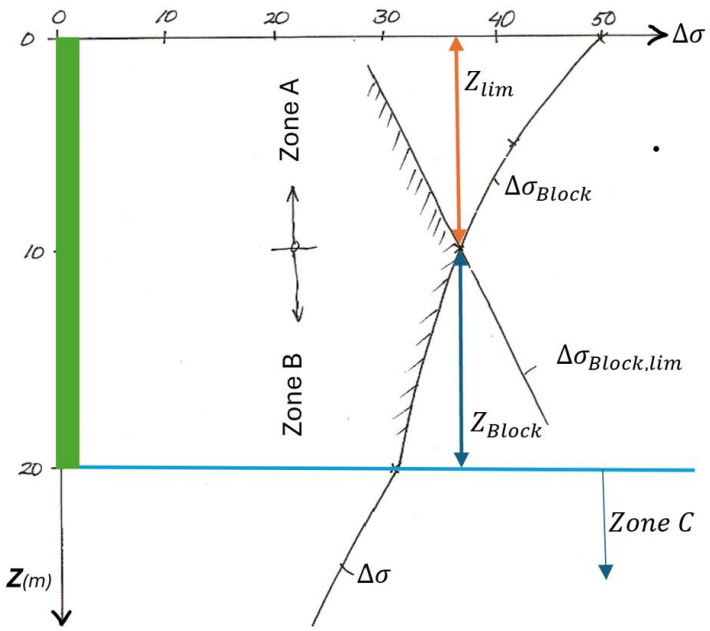

Figure 16 stress distribution modified from (Alén et al., 2005a)

The block strain:

$$\varepsilon_{block} = \Delta\sigma_{block}/M_{block} \quad \text{.....B 4}$$

Where $\Delta\sigma_{block}$ is the average stress increase in the block (Alén et al., 2005a).

According to the method assumption, in zone B the plane sections will remain plane, the corresponding stress increase is proportional to the stiffness.

$$\Delta\sigma_{soil} = \Delta\sigma_{block} \,.\, M_{soil}/M_{block} \quad \text{.....B 5}$$

$$\Delta\sigma_{col} = \Delta\sigma_{block} \,.\, E_{col}/M_{block} \quad \text{.....B 6}$$

The derivations of these equations are:

$$\varepsilon_{soil} = \varepsilon_{col} = \varepsilon_{block} \quad \text{.....B 7}$$

Where $\varepsilon_{soil},\ \varepsilon_{col}, and\ \varepsilon_{block}$ are the vertical strains in the soil, the columns, and the block.

That means the strain from zone A = The strain from zone B = The strain from zone C at the equilibrium. Figure (17) shows the stress distribution in soil zones. Where stresses are reduced by depth.

a b c

$$\frac{\Delta\sigma soil}{Msoil} = \frac{\Delta\sigma col}{Ecol} = \frac{\Delta\sigma block}{Mblock} \Rightarrow\Rightarrow\Rightarrow\Rightarrow$$

$$\alpha = b \Rightarrow \ \Delta\sigma col = \frac{Ecol}{Msoil} \,.\, \Delta\sigma soil \ , and \ \Delta\sigma block = \alpha.\Delta\sigma col + (1-\alpha)\Delta\sigma soil \quad \text{.....B 8.}$$

$$\alpha = c \Rightarrow \quad \frac{\Delta\sigma soil}{Msoil} = \frac{\alpha.\frac{Ecol}{Msoil}.\Delta\sigma soil + (1-\alpha)\Delta\sigma soil}{Mblock} \Rightarrow$$

$$Mblock = \alpha.Ecol + (1-\alpha)Msoil \quad \text{.....B 9}$$

$$b = c \Rightarrow \quad \Delta\sigma col = \frac{Ecol}{Mblock} . \Delta\sigma block \quad \text{.....B 10}$$

The improved soil settlement in zone B (Alén et al., 2005a).

$$\delta_B = (\Delta\sigma block . Zblock)/Mblock \quad \text{.....B 11}$$

3-1-Zone A fully plastic zone

The derivation of $\Delta\sigma_{col}$ estimates that the columns are so strong (stiff) in compression resistance, this means the induced stress is smaller than the compression of the columns (Alén et al., 2005a). The compression strength of the columns is insufficient to carry the elastic proportional part of the applied load, and the columns are in a plastic failure state. The upper part of the columns was often failed in plastic failure conditions (zone A), while the columns below (zone B) deformed elastically in conjunction with surrounding soil (Alén et al., 2005a). The column cohesion intercept is found to be proportional to the column undrained shear strength.

Assuming the stresses in the column cause long term failure of the column with known $ƒ_{LCC}$ and $\sigma`_{vo}$

$$\Delta\sigma_{col.pl} = ƒ_{LCC} - \sigma`_{vo} \quad \text{.....B 12}$$

$$\Delta\sigma_{soil} = (\Delta\sigma_{block} - \alpha . \Delta\sigma_{col.pl})/(1 - \alpha) \quad \text{.....B 13}$$

Where $\sigma`_{v0}$ is in situ effective stress (Alén et al., 2005a).

The extent of zones A and B can be derived as the stresses in the columns are equal at the border between zone A and zone B (Alén et al., 2005b). The basic principles to calculate the depth of the failure are:

1-Determining the potential action effect from the surface load applied to the soil block.

2-Detrmining the resistance generated by the compression strength of the columns.

3-Comparing action effects calculated from (1) to the resistance obtained from (2), this gives the depth where the potential action effect is equal to the resistance effect.

4-The action effects must be less or equal to the resistance effects.

The stress distribution is normally decreasing with depth, while the opposite is happening with resistance. (Alén et al., 2005b).

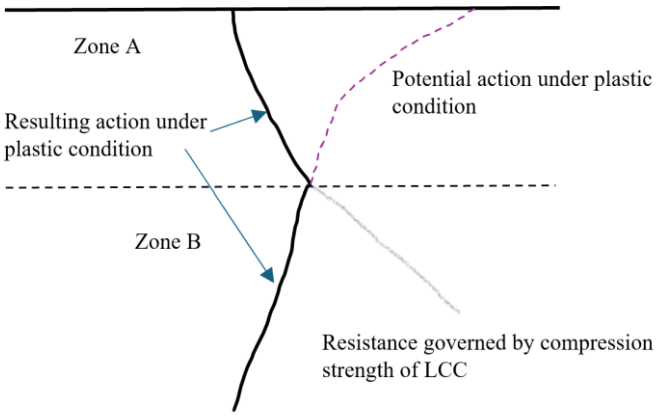

Figure 17 stress distribution in The Columns modified from (Alén et al., 2005b).

For firm bottom columns no stress distribution is accounted with depth, and the stress can be regarded constant with depth.

The *LCC* compression strength as an effective stress can be expressed:

$$f_{LCC} = K_{c`} \cdot c`_{col} + K_h \cdot \sigma`_h \quad \text{.....B 14}$$

$$K_{c`} = 2.tan\,(45^0 + \emptyset`/2) \text{.....B 15}$$

$$K_h = tan^2\,(45^0 + \emptyset`/2) \text{.....B 16}$$

The column cohesion intercept is found to be proportional to the column undrained shear strength.

$$c`_{col} = const\,.\,c_{u,col} = (0{,}4 - 0{,}45).\,c_{u,col} \quad \text{.....B 17}$$

For φ = 30̊ for columns and the value of const = √3/4 = 0,43 the columns compression strength is

$$f_{LCC} = 1{,}5\,.\,c_{u,col} + 3.\sigma`_{h,col} \text{.....B 18}$$

Where $C_{u,col}$ is the undrained, unconfined shear strength of the columns.

Further assumes relate:

$$\sigma`_h = K_0\,.\,\sigma`_{vo} + 0{,}5\,.\,\Delta\sigma`_{soil} \text{.....B 19}$$

where $\sigma`_{vo}$ is in situ effective stress. when K_o = (2/3) = 0.67 then the columns shear strength is:

$$f_{LCC} = 1{,}5\,.\,c_{u,col} + 2\,.\,\sigma`_{vo} + 1{,}5\,.\,\Delta\sigma`_{soil} \quad \text{.....B 20}$$

Where $\Delta\sigma`_{soil}$ is the increment of stress in soil due to surface loading.

At the zones border the extent of the elastic and plastic zone zones are equal

$$f_{LCC} = \sigma`_{col} = \sigma`_{col}(0) + \Delta\sigma`_{col} \text{.....B 21}$$

By inserting f_{LCC} from Equation (B20) and $\Delta\sigma`_{col}$ and $\Delta\sigma`_{soil}$ derived from elastic condition the in-situ stress in the columns and the soil are equal where $\sigma`_{col}(0) = \sigma`_{vo}$

The Equation (B20) can be written: (Alén et al., 2005b).

$$1{,}5\,.\,c_{u,col} + 2\,.\,\sigma`_{vo} + 1{,}5\,.\,\frac{M_{soil}}{M_{block}}\Delta\sigma_{block} = \sigma`_{vo} + \frac{E_{col}}{M_{block}}.\Delta\sigma_{block} \text{.....B 22}$$

Solving $\Delta\sigma_{block}$ gives the stress increment at the limit (border) between plastic zone A and elastic zone B, and the Equation (B21) is only valid at limits between the tow zones, figure (19). The Equation (B22) becomes:

$$\Delta\sigma_{block,lim} = \frac{1{,}5\,.c_{u,col} + \sigma`_{vo}}{E_{col} - 1{,}5\,.M_{soil}}\,.M_{block} \quad \text{.....B 23}$$

Equation B23 can be compared to the general expression of the stress increment which outlined at the main text:

$$\Delta\sigma_{block} = \eta_{LC}\,.\,q + (1 - \eta_{LC}).\,\frac{q\,.\,B}{B+z}. \quad \text{.....B 24}$$

Where B = width of surcharge. (Alén et al., 2005b). And η_{LC} is load distribution figure (18).

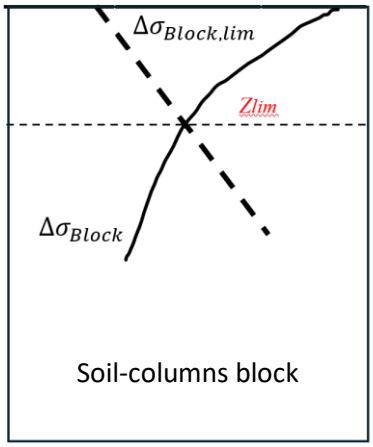

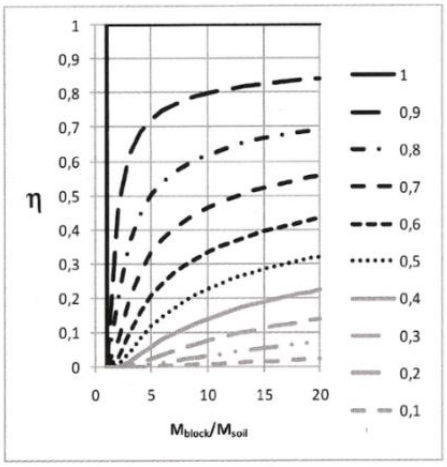

Figure 18 load distribution (Alén et al., 2005a).

Figure 19 limits between zone A, and Zone B modified from (Alén et al., 2005b).

For floating columns:

$$\eta_{LC} = (D/H)^{1/v} \quad \text{.....B 25}$$

Where H = the depth down to firm layer

D = length of the columns

$$v = (\frac{M_{block}}{M_{soil}})^{0.1} - (\frac{M_{soil}}{M_{block}})^{0.1} \quad \text{.....B 26}$$

Load distribution estimates:

one part of the external load $\eta_{LC} \cdot q$ is transmitted down straight to the bottom of the stabilized soil, the other part $(1 - \eta_{LC}) \cdot q$ is distributed with depth (2:1 – method) due to the elasticity theory. Figure (18) shows load distribution (Alén et al., 2005a). For firm bottom when the columns extend to firm layer $\eta_{LC} = 1$, and then $\Delta\sigma_{block} = q$ in Equation B24. Figure (20) shows the variation of η_{LC} with depth when for example Mblock/Msoil = 5.

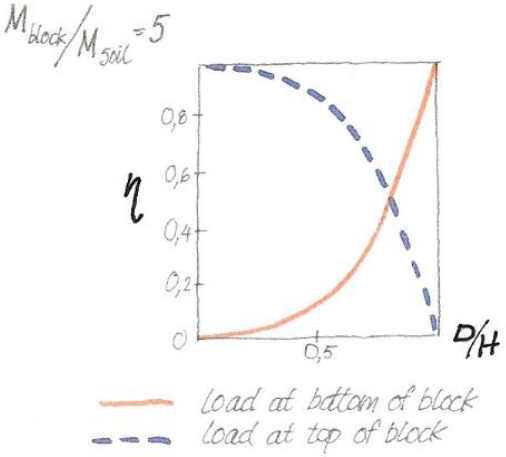

Figure 20 Variation of η_LC with depth for Mblock/Msoil =5 (Alén et al., 2005a).

Zlim can be deprived from the Equation:

$$\Delta\sigma_{block,lim} = \Delta\sigma_{block} \Rightarrow Z_{lim} \quad \text{.....B 27}$$

The extent of plastic zone can be found by deriving $\int_{LCC}$ and $\sigma`_{col}$ in Equation B21:

(Alén et al., 2005b).

$$\int_{LCC} = \frac{1{,}5 \cdot (1-\alpha) \cdot c_{u,col} + (2-0{,}5 \cdot \alpha) \cdot \sigma`_{vo}(z) + 1{,}5 \cdot \Delta\sigma_{block}(z)}{1+0{,}5 \cdot \alpha} = \sigma`_{col} = \sigma`_{vo} + \frac{E_{col}}{M_{block}} \cdot \Delta\sigma_{block}(z) \quad \text{.....B 28.}$$

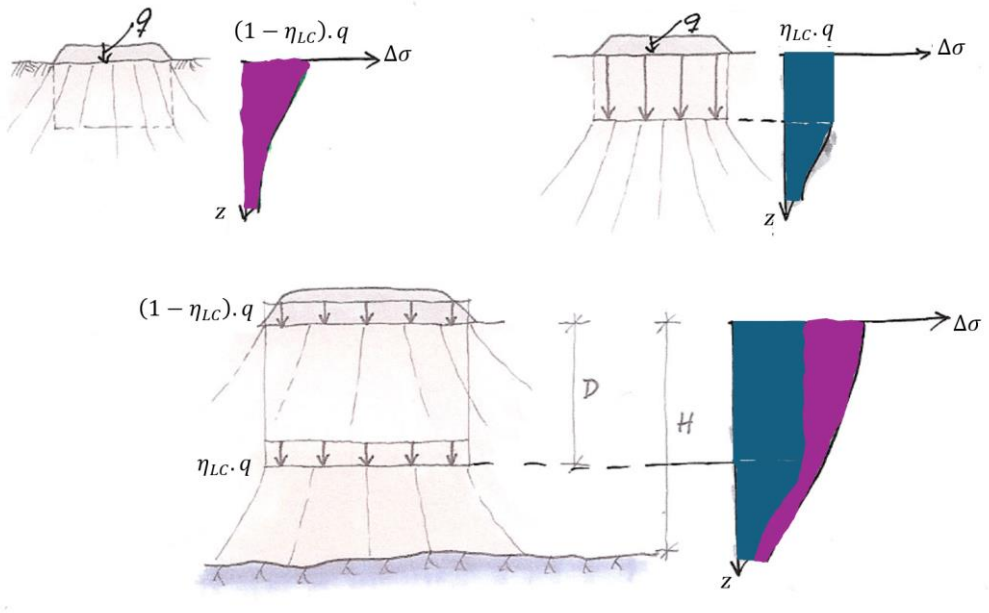

Figure 21 load distribution for floating columns modified from (Alén et al., 2005a).

3-1-1-Soil stresses and settlement in plastic zone A

The columns in plastic zone are in failure mode, and to calculate the settlement soil stresses needed to be calculated at the bottom of plastic zone A when z = z_{lim}, and the stresses equation is:

$$\Delta\sigma_{soil}(z_{lim}) = \frac{M_{soil}}{M_{block}} . \Delta\sigma_{block}(z_{lim}) \quad \text{.....B 29.}$$

At the top of the zone when z = 0 the compression strength in Equation B21 becomes:

(Alén et al., 2005b).

$$f_{LCC}(0) = 1{,}5 . c_{u,col} + 1{,}5 . \Delta\sigma`_{soil} \quad \text{.....B 30}$$

As $\sigma`_{vo} = 0$, and $\Delta\sigma_{block}(0) = q$, then the stress is: (Alén et al., 2005b).

$$\Delta\sigma`_{soil} = \frac{q-a.f_{LCC}}{1-a} \quad \text{.....B 31}$$

And the Equation B30 becomes:

$$f_{LCC}(0) = 1{,}5 . c_{u,col} + 1{,}5 . \frac{q-a.f_{LCC}}{1-a} \quad \text{.....B 32}$$

Solving B32 Equation calculates the *LCC* strength at the topsoil and columns surface:

$$f_{LCC}(0) = \frac{1{,}5}{1+0{,}5 .a} . [(1-a). c_{u,col} + q] \quad \text{.....B 33}$$

And B31 Equation at the topsoil surface becomes:

$$\Delta\sigma`_{soil}(0) = \frac{2 .q-3 .a.c_{u,col}}{2+a} \quad \text{.....B 34}$$

This equation is only valid when the columns are in the situation of plastic failure (Alén et al., 2005b).

For settlement calculations in the zone, an average soil stress increment from equations B29 and B34 can used: (Alén et al., 2005b).

$$\Delta\sigma`_{soil} = \frac{\Delta\sigma`_{soil}(0)+\Delta\sigma`_{soil}(z_{lim})}{2} \quad \text{.....B 35}$$

The settlement at the border limit point is given by: (Alén et al., 2005a).

$$\delta_A = \frac{\Delta\sigma`_{soil}}{M_{soil}} . z_{lim} \quad \text{.....B 36}$$

3-2-Soil stresses and settlement in zone C

This zone exists when the columns are floating and are not reaching a firm bottom layer, Where $\eta_{LC} < 1$. Figures (18, 21, and 22).

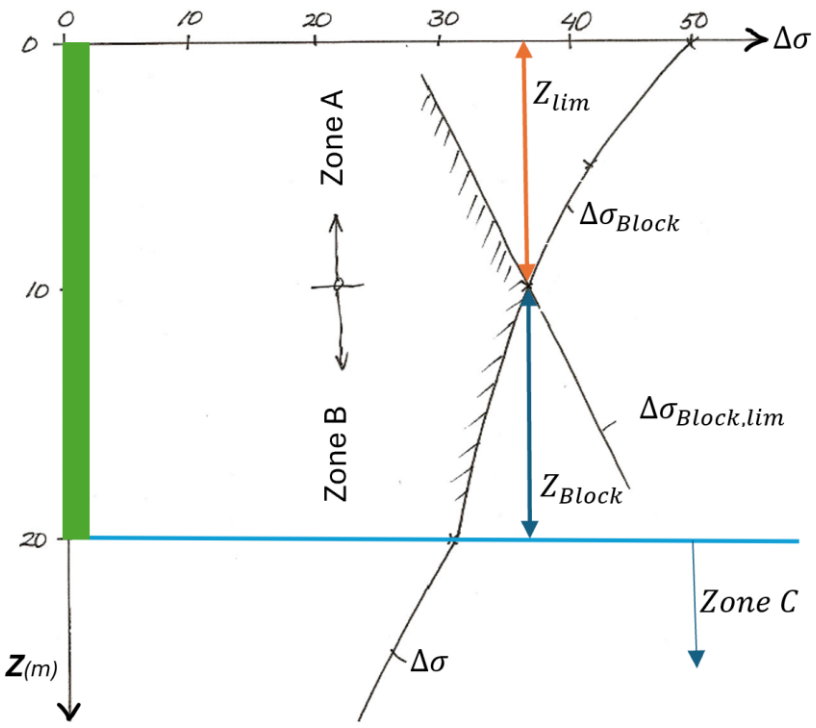

Figure 22 stress distribution modified from (Alén et al., 2005a).

The stresses in the soil beneath the stabilized soil can be calculated from the equation: (Alén et al., 2005a).

$$\Delta\sigma_{Zone\ C} = \frac{\eta_{LC} . q . B}{(B+(z-D))} + (1-\eta_{LC}). \frac{q . B}{(B+z)} \quad \text{.....B 37}$$

The settlement at zone C:

$$\delta_C = \frac{\Delta\sigma_{soil(C)}}{M_{soil}} . z_C \quad \text{.....B 38}$$

For Columns reaching firm layer there is no zone C and the calculating the settlements is somehow easier figure (23) as the following: (Alén et al., 2005a).

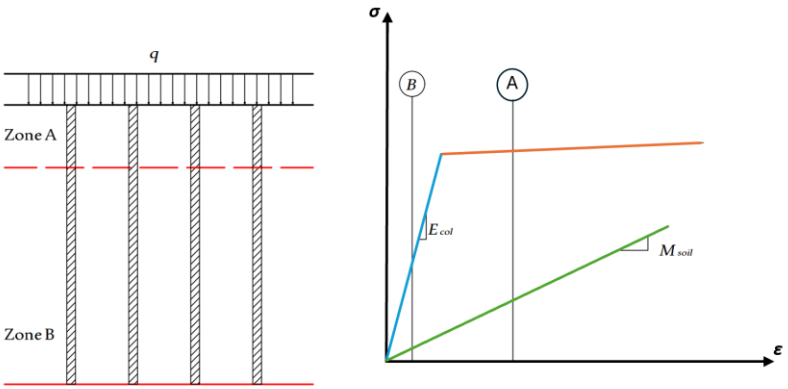

Figure 23 Stress Distribution when η=1 firm layer (Alén et al., 2005a).

1- Estimate columns diameter and spacing and calculate α depending on columns pattern.
2- Determine material properties M_{soil} , $Cu_{,col}$, E_{col} , and M_{block} .
3- $\eta = 1$ *then* $\Delta\sigma_{block,lim} = q$ *and* Z_{lim} *can be calculated.*
4- The equation B24 can be written $\Delta\sigma_{block,lim} = \frac{M_{block}\,.(1.5\,c_{u,col} + \sigma`_{vo})}{(E_{col} - 1.5\,M_{soil})}$
5- After calculating Z_{lim} zone A and Zone B can be illustrated.
6- Zone B settlement can be calculated $\delta_B = \frac{q}{M_{block}}\,.h_b$ *where* $h_b = H - h_A$.
7- Stress increase in zone A can be written from equations B30 and B35:
   $\Delta\sigma_{soil}(0) = \frac{2.q - 3.\alpha.c_{u,col}}{(2+\alpha)}$ and $\Delta\sigma_{soil}(z_{lim}) = \Delta\sigma_{block}(z_{lim})\,.\frac{M_{soil}}{M_{block}}$
   $\Delta\sigma_{soil} = [\Delta\sigma_{soil}(0) + \Delta\sigma_{soil}(z_{lim})]/2$ and $\delta_A = \frac{[\Delta\sigma_{soil}(0) + \Delta\sigma_{soil}(z_{lim})]}{2}\,.h_a$
8- The total settlement $\delta = \delta_A + \delta_b$
9- To evaluate the improvement the total settlement of none improved soil can be directly calculated from the equation: $\delta_{no\ improve} = \frac{q}{M_{soil}}.H$ where H is the total columns length inside the soil improved block.

3-2-Time dependent settlement

For clay Terzaghi consolidation equation can be used:

$\frac{\delta u}{\delta t} = c_v.\frac{\delta_u^2}{\delta_z^2}$ *where* $c_v = \frac{M\,.\,k}{\gamma_w}$ (Alén et al., 2005a). Terzaghi equation is valid for homogenous soil and for vertical flow, and it cannot be used directly for lime-cement stabilized soil because the columns have a higher hydraulic conductivity and a higher permeability than the clay soil. Usually from 500 to 1000 higher than soil (Vogler, 2008). The larger part of total stresses in the block will be transferred to the columns as the block continue to consolidate as well as the columns have a much higher stiffness than the clay soil (Alén et al., 2005a). Therefore, calculating the consolidation (time-settlement) of lime-cement stabilized soil by means of vertical drains is more valid. As a result, the most of the vertical flow of water occurs within the columns, while radial flow is induced from the soil toward the columns. To estimate this flow, we can use a calculation like that for vertical drains in clay. The degree of consolidation, U, is then given by: (Alén et al., 2005a).

$$U = 1 - exp\left(-\left(8\,.\frac{c_{h,block}}{d^2}\right).\frac{t}{\mu}\right) \quad \text{.....B 39}$$

Where $c_{h,block}$ is the horizontal coefficient of consolidation:

$$c_{h,block} = \frac{k_h \cdot M_{block}}{\gamma_w} \quad \text{.....B 40}$$

And μ is derived from vertical drain theory:

$$\mu = \frac{n^2}{n^2-1} \cdot \left[ln(n) - 0{,}75 + \frac{1}{n^2} \cdot \left(1 - \frac{1}{4 \cdot n^2}\right)\right] + \left(\frac{n^2-1}{n^2} \cdot \frac{4}{\emptyset^2} \cdot \frac{k_{soil}}{k_{col}} \cdot L_D^2\right) \quad \text{.....B 41}$$

where n is ratio between the equivalent diameter of influence D, and the diameter of the column ∅.

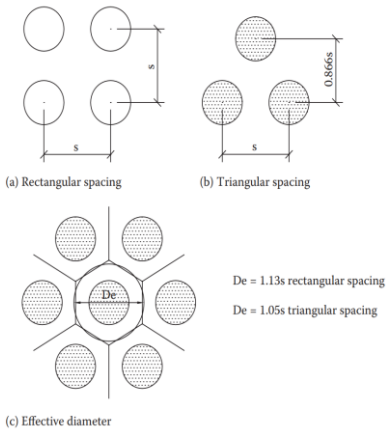

Figure 24 Ratio of improvement (Kirsch et al, 2012).

The final shape of B42 Equation can be written as:

$\mu = \mu_1 + \mu_2$ Where:

$$\mu_1 = \frac{1}{1-a} \cdot [ln\left(\sqrt{\frac{1}{a}}\right) - 0{,}75 + a \cdot \left(1 - \frac{a}{4}\right) \quad and \quad \mu_2 = (1-a).\frac{4}{\emptyset^2} \cdot \frac{k_{soil}}{k_{col}} \cdot L_D^2 \quad \text{.....B 42}$$

4-Design according to Eurocode 7

4-1-Ultimate limit state

Ultimate limit state (ULS) of Eurocode 7 estimates that the failure or collapse of the supported structures of the designed stabilised soil is unlikely to happen (Vogler, 2008). The overall stability of columns and the internal stability must be proved relevant and sufficient, and the excessive deformation of the whole structure or of parts of it are not allowed due to either the failure or the excessive deformations of the soil. The stability analysis is determined on the mean strength properties of both the untreated soil and the columns. Failure takes place along a plane or a curved plane due to the shear strength failure of columns and/or of the surrounding soil (EuroSoilStab ,2002).

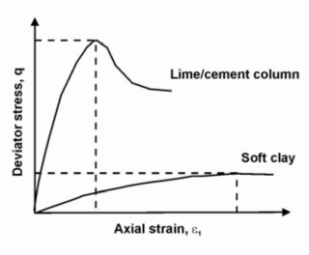

Figure 25 stress strain shape of columns and natural soil (Vogler, 2008).

Therefor the column shear strength must be restricted to approximately around 100 KN/m² in stability calculations, regardless of mixing tests results (EuroSoilStab ,2002). This restriction is to assure the full interaction of both soil and columns. The strength of an individual column must be determined from laboratory mixing tests. The in-situ shear strength of columns is approximately from 20-50% of the individual laboratory columns shear strength. The volume fraction of columns is then:

$$\Omega_c = \frac{A_{col}}{A} \qquad \ldots.C\ 1$$

Where A_{col} is the columns surface area, and A is the total surface area, as shown in figure (24). The design of required Ωc must be determined according to the combined and undrained analysis (Vogler, 2008). Combined analysis must take in account the lowest value of drained and undrained shear strength in all sections of possible slip surface. If the laboratory values were not performed the following design values can be estimated for columns: (Vogler, 2008)

$$c`_{k(col)} = \beta . c_{uk(col)} \qquad and \qquad \varphi`_{k(col)} = 30^0 \qquad \ldots\ldots\ldots C\ 2$$

Where $c`_{k(col)}$ and $. c_{uk(col)}$ are the drained and undrained cohesion of the columns. And $\varphi`_{k(col)}$ is the effective friction angle of the column. In our example $\varphi`_{k(col)} = 37^0$. β values depend on the position of the columns. Where β = 0.3 in the active shear zone. β = 0.1 in the direct shear zone. β = 0 in the passive shear zone (Vogler, 2008). The effective cohesion $c`_k$ and the drained shear strength τ_{fdk} of the improved block can be calculated:

$$c`_k = \Omega_c . c`_{k(col)} + (1 - \Omega_c) . c`_{k(soil)} \qquad \ldots\ldots C\ 3$$

$$\tau_{fdk} = c`_{k(col)} + \sigma` tan\varphi`_k \qquad \ldots\ldots C\ 4$$

Where $c`_{k(soil)}$ is the soil effective cohesion, σ` is the effective stress on slip surface. The effective friction angel $\varphi`_k$ is the same of soil and columns and improved block ( $\varphi`_k = \varphi`_{k(col)} = \varphi`_{k(soil)}$). With the same approach the undrained analysis can be calculated:

$$c_{uk} = \Omega_c . c_{uk(col)} + (1 - \Omega_c) . c_{uk(soil)} \qquad \ldots\ldots C\ 5$$

$$\tau_{uk} = c_{uk} \qquad \ldots\ldots C\ 6$$

The stability calculations above were based on the estimation of full interaction between columns and the surrounding soil, which is not always relevant. In case of creep circumstances in clay this interaction is not valid (Vogler, 2008).

4-1-Serviveability limit state

Serviceability limit state requirements should be specified by the client criteria, settlements are most referred and defined by clients inquiry during the service life of structure (Vogler, 2008). Structure settlements calculations of columns group are based on the assumption that the axial deformation of the columns is the same as the deformation of unstabilised soil between columns. And the vertical strains at a certain depth are equal in both columns and the surrounding unstabilised soil. The columns group settlement is determined by the weighted average compression modulus of the columns and the surrounding soil. The calculated model estimates that the soil is horizontally layered and that the columns have the same depth. More than one depth of columns can be used depending on the settlement values and the soil properties (Vogler, 2008). If columns of varied length were used the settlement calculations must be calculated for each length. This variation gives the advantage of the increase of compression modulus and of undrained shear strength. The total load q is distributed between soil and columns on the assumption that the same compression happens in columns and surrounding soil at every depth. That means the soil load q_{soil} will gradually be transmitted to the columns q_{col}, Figure (26).

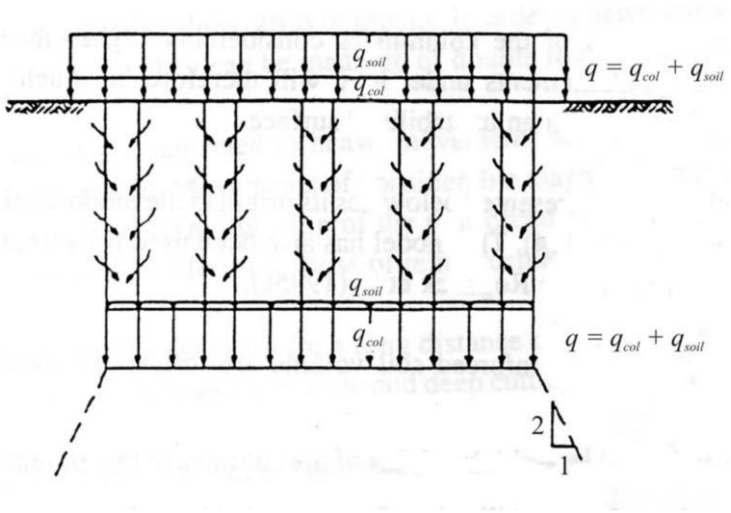

Figure 26 load distribution (Vogler, 2008).

The load displacement shape of the columns is estimated ideal elastic relating the long-term stress $\sigma`_{creep}$ with Young modulus $E_{col}$. Where $\sigma`_{creep}$ is not the time dependent constitutive behaviour of creep, but instead it is limiting the vertical stress to a stress level at which no time dependent strains will happen (Vogler, 2008). After reaching long-term stress $\sigma`_{creep}$ the columns will behave perfectly plastic. The load displacement shape of surrounding unstabilised clay soil is estimated to be linear elastic with soil confined compression modulus $M_{soil}$. The ultimat strength $\sigma`_{ult}$ of the columns is:

$$\sigma`_{ult} = 2c_{uk} + 3\sigma`_{h} \qquad \text{.....C 7}$$

Where $\sigma`_h$ with is the horizontal effective stress between soil and columns. Equation C7 is determined on the assumption of $\varphi`_{k(col)} = 30^0$ (in this thesis $\varphi`_{k(col)} = 37^0$), and a total stress analysis (Vogler, 2008). The maximum designed load of individual columns $q_{col,max}$ is:

$$q_{col,max} = 0.9 \,.\, \Omega_c \,.\, \sigma`_{ult} \qquad \text{.....C 8}$$

Then the remained load will be loaded to the soil:

$$q_{soil} = q - q_{col} \qquad \text{.....C 9}$$

The settlement can be written:

$$S_{col} = \sum \frac{q_{col}.\Delta h}{\Omega_c \,.E_{col}} \quad and \quad S_{soil} = \sum \frac{q_{soil}.\Delta h}{(1-\Omega_c) \,.M_{soil}} \qquad \text{.....C 10}$$

Where S_{col} and S_{soil} are the soil and columns settlements, E_{col} is columns Young modulus, and M_{soil} is the confined soil compression modulus. M_{soil} is always stress dependent (Vogler, 2008). The guidelines consider that the relatively stiff columns can bunch against the supporting soft soil, while the soil is constrained by using M_{soil} to calculate soil settlements. At the same time the in-situ soil is relatively soft, and it will normally consolidate with no given high lateral support to the column's materials. By using E_{col} instead of one-dimensional compression modulus for columns the slight bulging of columns materials will be taken in account and $S_{col} > S_{soil}$. The calculation of total settlements S is an iterative process, by assuming that $q_{col} = q_{col,max}$ then calculating the columns and soil settlements S_{col} and S_{soil}. If $S_{col} > S_{soil}$ a load will transfer from columns to soil for next iteration. If $S_{col} < S_{soil}$ the columns are loaded up for long term load, and they cannot take any more load. Then the resulted settlement $S = S_{soil}$. For normally consolidated clay the settlement is:

$$S = S_{col} = S_{soil} = \sum \frac{q.\Delta h}{\Omega_c \,.E_{col} + (1-\Omega_c) \,.M_{soil}} \qquad \text{.....C 11}$$

For floating columns the settlement calculations for soil below columns can be estimated by any conventional settlement calculation methods (Vogler, 2008).

5-Volume averaging techniques (VAT)

5-1-Introduction

Volume averaging techniques is a method using finite element software Plaxis analysis for modelling deep mixing stabilized soil consisting of soil material and deep mixed stabilizing binder columns material. This method converts a composite model of soil and deep mixing columns as aperiodic system into a homogenous material instead of modelling the natural soil and the deep mixed columns separately (Becker, Karstunen, 2013). Volume averaging techniques assumes a periodic distribution of the columns in the soil and a perfect bonding between soil and deep mixed columns with no slip occurrence between columns and the natural soil. It is a homogenisation method, averaging tow independent constitutive models of ground improved columns and soil (Vogler, 2008). Soil reinforced by means of columnar inclusion can be considered as a composite material and can be modelled as a homogenous but anisotropic continuum, taking in account the geometrical regularity of the columns and the different mechanical and physical properties of the soil and the columns (Vogler, 2008). This approach simplifies the problem, and enables the solution based on finite element method. Figure (27).

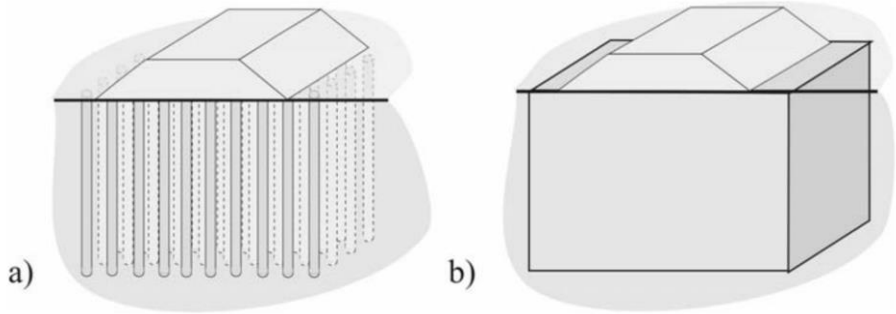

Figure 27: a) discrete, b) homogenised visualisation of embankment problem solving (Vogler, 2008).

Accurate prediction of stress distribution between soil and columns needs a certain mesh fineness, so a high number of volume elements is even more important to achieve this accurate prediction. This method is matching the design purposes and enables any change in columns diameter and spacing without changing or drawing a new geometric discretisation of the problem by changing only Ωc parameter in Plaxis (Vogler, 2008). The used finite element mesh is independent of the dimensions and the spacing of the columns and simple. Soil and columns will be modelled in volume averaging method by tow individual constitutive models. Any constitutive model of elasto-plastic constitutive material can be used, and the parameters of the constitutive model can be derived from standard elementary laboratory tests of the soil and the columns (Vogler, 2008). Soft soil can be simulated using S-CLAY model which is a type modified from Cam Clay model. This type of clay can predict the anisotropic soil behaviour and the effects of interparticle bonding and destruction (Vogler, 2008). Columns can be simulated as MNhard type, this type can simulate the hyperbolic stress-strain behaviour of deep mixing columns, the different primary loading and unloading-reloading stiffness, the stress dependent stiffness, and the Matsuka-Nakai failure criterion. Numerical methods using finite element (FE) offer an alternative approach to conventional methods, particularly when they are calculating serviceability limit state, such as deformation analysis under working loads. FE analysis can incorporate advanced constitutive models to accurately predict the complex stress-strain behaviour of natural soil and stabilized columns (Becker and Karstunen, 2013). Several authors proposed numerical modelling approaches for homogenised material of columnar improved soil, in this thesis, we took the Vogler

Karstunen approach. In volume averaging method a 3D problem analysis can be simulated as 2D by simulating the column-improved soil as a homogenous composite material, and by using clever mathematics to map the true 3D problem into 2D (Becker, Karstunen, 2013). This conversion simplifies the solution period taken by Plaxis software.

5-2-Constitutive modelling

A constitutive modelling refers to the mathematical series of expressions for stresses and strains rate and conditions which are used to model the behaviour of an element and its material (Lees, A, 2016). This constitutive modelling must guarantee the equilibrium and compatibility between each element and allows complex problems to be analysed and stresses and displacements to be calculated at any estimated construction stage in every place of the estimated model. FE analysis can simulate a lot of complex soil structures and ground behaviour interaction problems, but the accuracy of this simulation depends heavily on the correct constitutive models assigned to each material and element (Lees, A, 2016). In any soil-structure analysis soils are usually the weakest and the softest material, therefore the soils behaviour determines the most deformations and the probability of failure. It is important to model their behaviour precisely over the range of strains and stresses they will experience in an appropriate constitutive model. While construction materials like steel, concrete, and binders are much stiffer than soils and can be modelled with simple linear elastic constitutive modellings (Lees, A, 2016). Cam Clay constitutive models were invented and modelled by Roscoe 1958 to simulate clay soils. These models were developed to the Modified Cam Clay by Roscoe and Burland 1968 and later on it has been developed towards more advanced models up to the anisotropic de-structuration S-CLAY1S model (Vogler 2008).

5-2-1-S-CLAY1S

S-Clay1S is a developed model from isotropic modified cam clay. It is an extension of S_CLAY1 model (Koskinen et al., 2002). Additionally, it is an extension of the conventional critical state models by incorporating anisotropic plastic behaviour via an inclined yield surface. It employs a hardening law to simulate the formation or the erasure of fabric anisotropy during plastic deformation and straining (Karstunen et al., 2006). The yield surface equation is:

$$f = \frac{3}{2}[\{\sigma_d - p`\alpha_d\}^T \{\sigma_d - p`\alpha_d\}] - \left[M^2 - \frac{3}{2}\{\alpha_d\}^T\{\alpha_d\}\right].(p`_m - p`).p` \quad \text{.....(1}$$

Where σ_d is the deviatoric stress tensor. α_d is a deviatoric fabric tensor. Furthermore, it is a dimensionless second order tensor that analogously is defined to deviatoric stress tensor (Wheeler et al., 2003). M is the critical state stress ratio. While $p`_m$ contributes the size of the yield surface of natural clay. Figure (28a) shows the three-dimensional shape of the yield surface for S-CLAY1S.

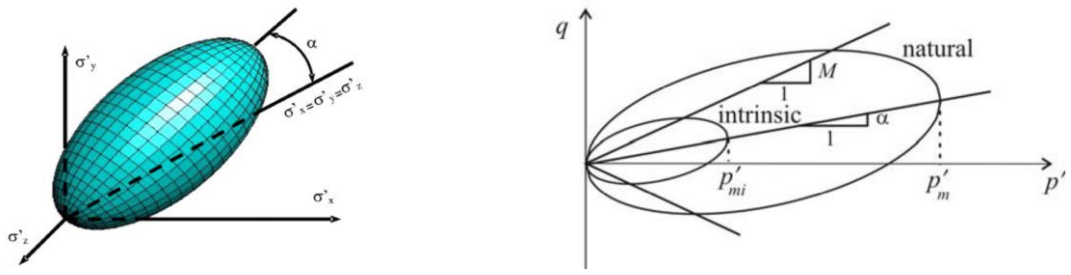

Figure 28 a) 3D S-CLAY1S yield surface (Karstunen et al., 2006). (b) natural and intrinsic yield curves (Vogler, 2008).

The intrinsic yield surface represents the notional yield surface for the equivalent unbonded soil sharing the same fabric and the same void ratio as the real yield surface but in smaller scale. The intrinsic yield

surface size is determined by $p`_{mi}$ which is related to natural soil yield surface $p`_m$ by parameter *x* to define the degree of current bonding. Figure (30b):

$$p`_m = (1 + x).p`_{mi} \qquad \text{.....(2}$$

Where *x* the bonding amount refers to difference size between bonded and unbonded yield surface. For simplification, it can assume that the horizontal plane in triaxial test sample concurs with the plane of isotropy of the sample and the parameter α can be defined as

$$\alpha^2 = \frac{3}{2}\,[\{\alpha_d\}^T.\,\{\alpha_d\}] \qquad \text{.....(3}$$

S-CLAY1S associates with three hardening laws (Koskinen et al., 2002). The **first law** relates the increment of plastic volumetric strain, $d\varepsilon_v^p$, to the increase of the size in the unbonded intrinsic yield surface. This first law assumes the increase of an unbonded soil yield surface is only due to the rearrangement of the soil particles into a denser shaping volume during the plastic strain occurrence (Karstunen et al., 2006).

$$dp`_{mi} = \frac{(1+e)p`_{mi}}{\lambda_i - \kappa}\, d\varepsilon_v^p \qquad \text{.....(4}$$

Where λ_i , κ are relating to the intrinsic compression and swelling lines in $e\ -\ \ln p`$ plane.

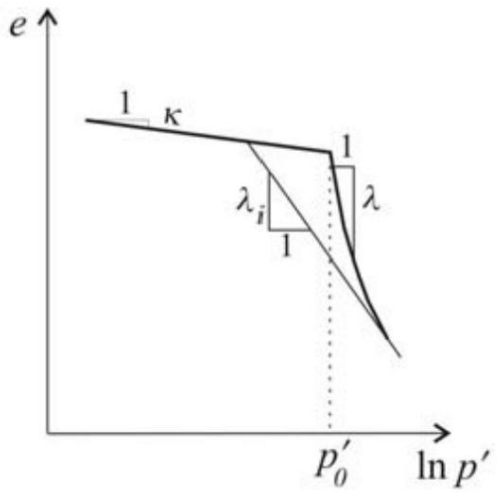

Figure 29 Compression of natural and reconstituted soil (Vogler, 2008).

The **second hardening law** defines the change of the yield surface orientation with plastic strain (Wheeler et al., 2003).

$$d\alpha_d = \mu\left(\left[\frac{3\eta}{4} - \alpha_d\right]\langle d\varepsilon_v^p\rangle + \beta\left[\frac{3\eta}{4} - \alpha_d\right].d\varepsilon_d^p\right) \qquad \text{.....(5}$$

Where $\eta = \alpha_d/p`, and\ \ d\varepsilon_d^p$ is the plastic deviatoric strain increment and μ and β are constants related to the soil. β controls the plastic shear strain and plastic volumetric strain relative effectiveness ratio in the overall sitting of instantaneous target values of the components of α_d (Wheeler et al., 2003). Whereas μ controls the absolute rotation rate of the yield surface with the current values of the components of σ_d. The **third hardening law**, the destructuation explains the degradation and rearranging of soil bonding with plastic straining. This is in somehow has a similar form to equation (5), except both negative or positive plastic shear and plastic volumetric strains decrease the value of bonding towards zero (Karstunen et al., 2006):

$$dx = a\left([0 - x].\left|d\varepsilon_v^p\right| + b[0 - x].d\varepsilon_d^p\right) = -ax\left(\left|d\varepsilon_v^p\right| + b.d\varepsilon_d^p\right) \text{.....(6}$$

α and b are additional soil constants. α refers to the absolute rate of destructuation. And b refers to the plastic deviatoric strains and plastic volumetric strains relative effectiveness in destroying the soil bonding (Koskinen et al., 2002). Equation (6) shows any small reduction in x parameter may result in reduction of $p`_m$ and furthermore it may decrease the peak undrained shear strength of the soil. This behaviour were evident during field tests and observations on moderately sensitive Finnish clays (Karstunen et al., 2005). If state parameter x reduced to zero and λ value, which can be deprived from a normal oedometer experiment test for the natural clay sample were used instead of intrinsic λi, the S-CLAY1S constitutive model will be converted to S-CLAY1. Where S-Clay1 accounts better for plastic anisotropy. If the initial values of α and μ value were set to zero the constitutive model will be converted to an isotropic modified Cam-Clay MCC (Karstunen et al., 2006). The determination of state parameters and soil constants values in S-CLAY1 are clear and straightforward (Wheeler et al., 2003). For S-CLAY1S an oedometer test is required for the reconstituted sample to define λi, and a sensitivity measure is required to estimate x value (Koskinen et al., 2002).

Parameter	description
κ	Swelling index in e - ln p' space
λ	Intrinsic compression index in e - ln p' space
ν	Poisson's ratio
M_c	Critical state stress ratio (stiffness)
ω	Auxiliary time integration
ω_d	
e_o	Initial void ratio
α_o	Initial yield surface inclination
x_o	Initial amount of bonding
OCR	Over consolidation ratio OCR = $\sigma`_p$ /$\sigma`_z$
POP	Pre overburden pressure POP = $\sigma`_p$- $\sigma`_z$
ξ	Absolute rate of destructuration
ξd	Relative effectiveness of destructuration

Table 4 S-CLAY1S input parameters

5-2-2-Constitutive column model: MNhard

MNhard model were formulated from the classic theory of plasticity within hardening soil model (HS) (Benz, 2007). The total strains is assumed considering stress dependent stiffness for elastic unloading, reloading and primary shear loading considering a non associated flow rule (Leoni, 2009). Failure criterion is provided by Matsuka and Nakai (Matsuoka and Nakai, 1982). This failure criterion is more closer to the observed failure for granular materials compared with Mohr-Coulomb criterion. The pre-failure attitude of serviceability limit state is independent from the failure criterion (Leoni, 2009). The hyperbolic stress strain relationship shown in figure (30a).

Figure 30 a) Hyperbolic stress-strain relationship, (b) Matsuka-Nakai (MN) and Mohr-Coulomb (MC) Failure criterion (Vogler, 2008).

The employed model is categorized as hardening plasticity model. Where the yield surface is not fixed to the principal stress path, rather it can expand due to plastic deformations figure (30b). Typically, tow primary types of hardening are recognized: shear hardening and compression hardening. Shear hardening for modelling the irreversible strains due to primary deviatoric loading (Vogler 2008). Compression hardening, on the other hand, for modelling irreversible strains due to primary compression in isotropic and one-dimensional loading. One dimensional is considered of minor importance as the stress paths in columns under loading are steep and the columns can extend laterally towards the soft soil ($\eta > \eta_{k_0}$) (Vogler 2008). The Matsuka-Nakai secant stiffness are stress dependent and it is defined as:

$$E_{50} = E_{50}^{ref} \cdot \left(\frac{c` \cos\varphi` - \sigma`_3 \sin\varphi`}{c` \cos\varphi` - p`_{ref} \sin\varphi`} \right)^m \quad \text{.....(7}$$

And the yield function is:

$$f = \frac{3}{2} \frac{1}{E_{50}} \frac{\left(\frac{1-\sin\varphi`_m}{\sin\varphi`_m}\right)}{\left(\frac{1-\sin\varphi`_m}{\sin\varphi`_m}\right) - R_f\left(\frac{1-\sin\varphi`}{\sin\varphi`}\right)} - \frac{3}{2} \frac{q}{E_{ur}} - \gamma_s^{ps} = 0 \quad \text{.....(8}$$

Where γ_s^{ps} is the hardening parameter and the plastic part of objective shear strain (Brinkgreve , 2002). $\varphi`_m$ is the mobilised friction angle, and R_f is the failure ratio between the ultimate deviatoric stress and the asymptote strain figure (30a). And it can be set $R_f = 0.9$ as a default value (Brinkgreve , 2002). As the MNhard model is a plasticity hardening model, the yield surface can expand due to plastic straining because it is not fixed in the principal stress surface (Vogler 2008). *m* represents the amount of stress dependency power, for clays 0.5<m<1.0 (Von Soos, 1990). *Eur* the module of unloading-reloading is three times *E50* , which can deprived from Fig (32a). E_{50}^{ref} can be deprived from Equation (7). Dilatancy ψ only accounts when if $\varphi`_m \geq \frac{3}{4} \varphi`$ (Vogler 2008). For lower $\varphi`_m$ values dilatancy $\psi = 0$.

Parameter	Description
$c`$	Effective cohesion
$\varphi`$	Effective friction angle
$\nu`$	Poisson's ratio at drained conditions
$\psi`$	Effective dilatancy angle
G_{ref}^{ur}	Reference shear modulus for unloading/reloading
m	Power of hyperbolic stress-strain law
G_{ref}^{50}	Reference shear modulus for primary loading
$p`_{ref}$	Reference pressure for hyperbolic stress-strain law
R_f	Ratio of failure
Ω	Volume ratio

Table 5 MNhard Parameters

5-3-Equivalent material stiffness matrix

A periodic distribution of columns within the soil is assumed as a homogenous material instead of modelling the natural soil and the columns separately (Becker, Karstunen, 2013). It assumes a perfect bonding and no slip between the soil and the columns figure (31).

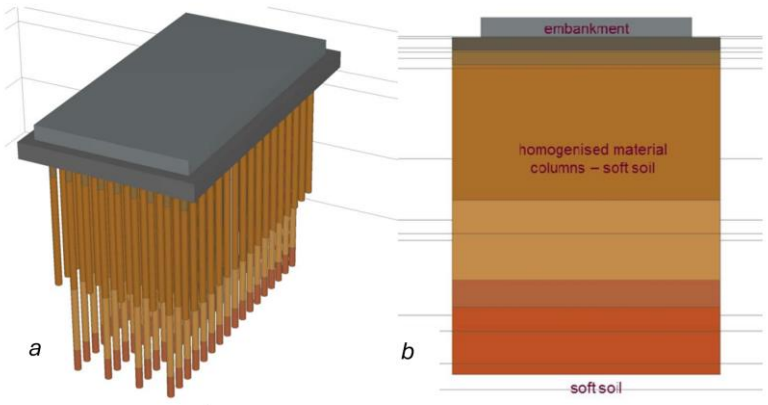

Figure 31 Discrete, (b) homogenised representation of embankment problem (Becker, Karstunen, 2013)

This allows adopting of any elasto-plastic constitutive model to the tow constituents materials: improved and natural soil (Becker, Karstunen, 2013). Homogenisation is carried out by determining the stresses and the strains increments of the homogenised equivalent material according to the following equations:

$$\dot{\boldsymbol{\sigma}}^{eq} = \Omega_s . \dot{\boldsymbol{\sigma}}^{s} + \Omega_c . \dot{\boldsymbol{\sigma}}^{c} \qquad \text{.....Eq 1}$$

$$\dot{\boldsymbol{\varepsilon}}^{eq} = \Omega_s . \dot{\boldsymbol{\varepsilon}}^{s} + \Omega_c . \dot{\boldsymbol{\varepsilon}}^{c} \qquad \text{.....Eq 2}$$

Where Ω refers to volume fraction, the superscripts eq, s, and c refer to the homogenised material (Becker, Karstunen, 2013). $\dot{\sigma}$ and $\dot{\varepsilon}$ are the total stress and strain rate tensors. Y-axis is assumed in the vertical direction in the following. The initial assumption of the local equilibrium between soil and the column material in each integration point can be written with the assumption that there is no stress discontinuity between soil and column material in terms of shear and radial stress as shown in figure (32).

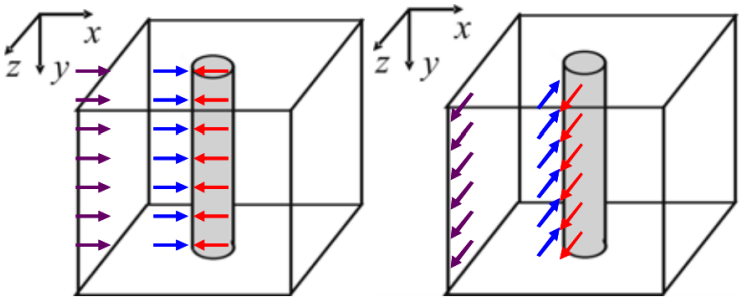

Figure 32 Local Equilibrium conditions between soil and column for a) Radial, (b) Shear stress (Becker, Karstunen, 2013).

$$\dot{\sigma}_x^{eq} = \dot{\sigma}_x^{s} = \dot{\sigma}_x^{c}$$

$$\dot{\sigma}_z^{eq} = \dot{\sigma}_z^{s} = \dot{\sigma}_z^{c}$$

$$\dot{\tau}_{xy}^{eq} = \dot{\tau}_{xy}^{s} = \dot{\tau}_{xy}^{c} \qquad \text{.....Eq 3}$$

$$\dot{\tau}_{yz}^{eq} = \dot{\tau}_{yz}^{s} = \dot{\tau}_{yz}^{c}$$

The assumption of no slip between soil and columns means the vertical and the shear strain are the same in both the soil and the columns and can be translated to the following kinematic equations, figure (33).

$$\dot{\varepsilon}_y^{eq} = \dot{\varepsilon}_y^{s} = \dot{\varepsilon}_y^{c}$$

$$\dot{\gamma}_{zx}^{eq} = \dot{\gamma}_{zx}^{s} = \dot{\gamma}_{zx}^{c} \quad \text{.....Eq 4}$$

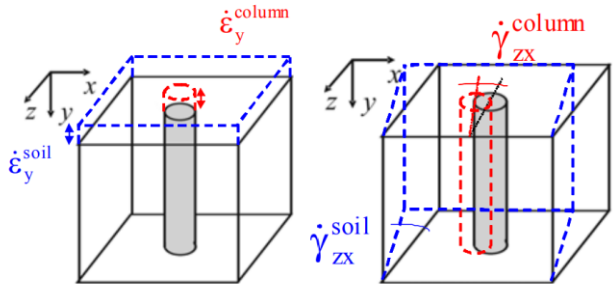

Figure 33 Kinematic perfect bonding between column and soil for (a) axial, (b) shear strain(Becker, Karstunen, 2013).

The constitutive equations for both constituents, the soil, and the columns regarding the increments of effective stresses are:

$$(\dot{\boldsymbol{\sigma}}^{s})` = \boldsymbol{D}^{s}\,\dot{\boldsymbol{\varepsilon}}^{s} \quad \text{.....Eq 5}$$

$$(\dot{\boldsymbol{\sigma}}^{c})` = \boldsymbol{D}^{c}\,\dot{\boldsymbol{\varepsilon}}^{c} \quad \text{.....Eq 6}$$

Where $\mathbf{D}^{cs}$ denotes the appropriate (elastic) or elasto-plastic stiffness matrices of the soil and the columns. For constituent material the soil modelled as S-Clay1S and the columns with MNhard (Becker, Karstunen, 2013). The averaged material constitutive equation -after considering the averaging rules at Eq 2 & Eq3 and inserting the kenimatic conditions in Eq 4 & Eq 5 -is:

$$(\dot{\boldsymbol{\sigma}}^{eq})` = \boldsymbol{D}^{eq}\,\dot{\boldsymbol{\varepsilon}}^{eq} \quad \text{.....Eq 7}$$

And the equivalent stiffness matrix can be wirriten:

$$\boldsymbol{D}^{eq} = \boldsymbol{\Omega}_s\,\boldsymbol{D}^{s}\,\boldsymbol{S}_1^{s} + \boldsymbol{\Omega}_c\,\boldsymbol{D}^{c}\,\boldsymbol{S}_1^{c} \quad \text{.....Eq 8}$$

The volume fraction ratio Ω is: (Vogler 2008)

$$\boldsymbol{\Omega}_c = \frac{A_c}{A} \quad \& \quad \boldsymbol{\Omega}_s = \frac{A_s}{A} \;;\; \boldsymbol{\Omega}_s = 1 - \boldsymbol{\Omega}_c \quad \text{.....Eq 9}$$

Where Ac and As are the cross-section area for columns and soil see figures (15, 16, and 26). For Square pattern. The column fraction ratio as shown in figure (15) is:

$$\boldsymbol{\Omega}_c = \frac{\pi . r_c^2}{c^2} = \frac{\pi . d^2}{4 . s^2} \quad \text{.....Eq 10}$$

Where d is the columns diameter and s is the columns spacing. For triangular and hexagonal pattern the column fraction ratio has different equation see (Vogler 2008) for more details.

Figure (34) shows the conceptual model of used defined model (UDSM) model used in plaxis

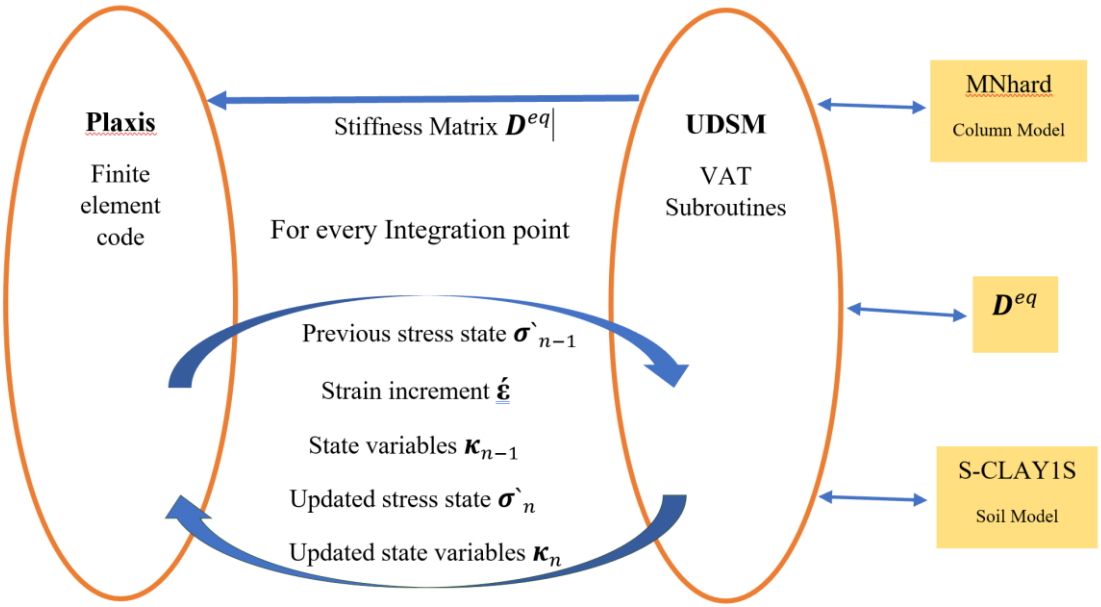

Figure 34 Concept of used defined soil model (USDM) modified from (Vogler, 2008).

6-A numeric application

The application is for an embankment on soft clay soil as shown in figure (35) below:

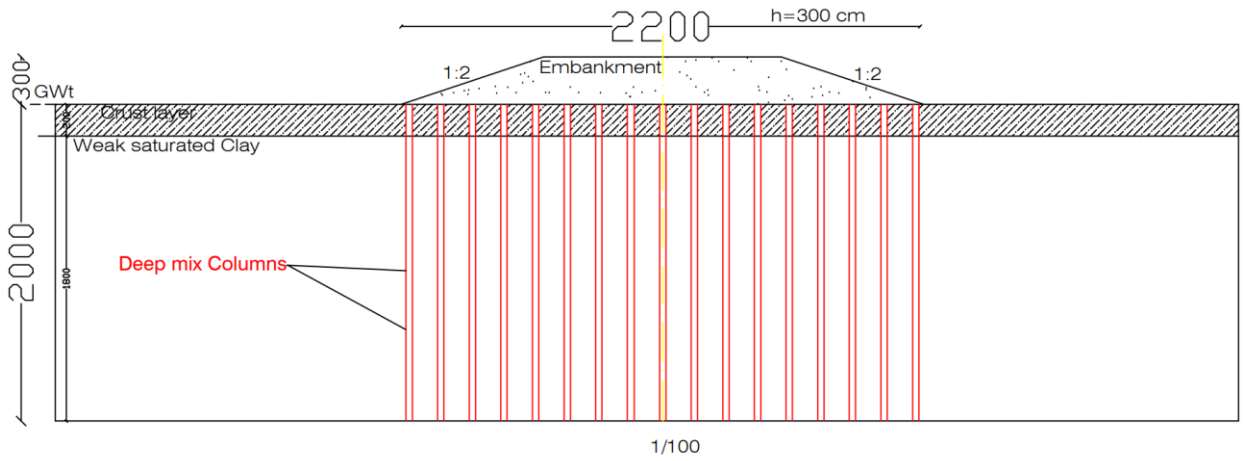

Figure 35 embankment stratigraphy.

A virtual embankment on soft soil clay were estimated. The soil geometry consists of a dry crust layer with 2m of depth and a weak saturated clay layer with 18m of depth settled on sandy moraine soil which is considered as firm layer for soil improved columns. The ground water table is located at the top of, dry crust layer. A soil model was estimated, and typical soil properties were assumed. Several spacings were calculated for tow column diameters to show differences of the results according to the variation of columns diameters and columns spacings. The following solve in chapter (6-1) will show numeric solving of Swedish method for only one diameter and one spacing D = 0.6m and c/c = 1m. Excel were

used to enable the comparison of results in Swedish method when the column diameters or spacings is changed. The following tables show the soft clay layer, the top dry crust layer, and the embankment parameters.

Parameter		**Unit**	**Description**
h	3	m	Embankment height
γ_b	14.2	KN/m³	Clay soil bulk density
ɣsat	14.2	KN/m³	Clay soil saturated density
κ	0.165		Swelling factor
λ	1.376		Compression factor
ν`	0.17		Poisson ratio
Mc	1.17		Critical state stress ratio in triax compression
Me	0.84		Critical state stress ratio in triax extension
Φ`	29.31		Clay effective friction angle
ψ	0		Dilatancy
POP	18	KN/m²	
e_o	3.34		Initial void ratio
K_oNC	0.51		Value at yield
$K_ox = K_oz$	0.638		In situ values
k_x	1.56e-4	m/day	Horizontal hydraulic conductivity
k_z	1.3e-4	m/day	Vertical hydraulic conductivity
C_k	1.5		Change in permeability

Table 6 Soil inputs for plaxis.

Model	**Mohr-Coulomb**			
	Unit	Dry Crust	Sandy Moraine	Embankment
ɣb	KN/m³	17	19	20
ɣsat	KN/m³	17	19	20
E	KN/m²	4077	40000	40000
ν (nu)		0.2	0.2	0.35
C ref	KN/m²	20	2	2
ϕ°	°	5	40	40
ψ	°	0	0	0
$k_\circ$ x		0.9128	0.36	0.36
$k_\circ$z		0.9128	0.36	0.36
kx	m/day	0.0013	1	1
kx	m/day	0.0013	1	1

Table 7 Dry crust and Embankment parameters.

sample	**12**	**13**	**14**	15	avarage
M0	**0.92**	**1.10**	**1.30**	1.35	1.17
ML	**0.38**	**0.28**	**0.30**	0.70	0.42
σ´c	**41.45**	**51.95**	**54.1**	80	56.9

Table 8 soil stiffness for Swedish method

6-1- Application solved with Swedish method

Embankment height h=3m, Embankment width B=22m Calculated from slope height and drift 1:2. Embankment bulk density ɣb =20 kN/m³.

Embankment load q= ɣb.h = 20. 3 = 60 Kpa.

Assuming that:

Columns diameter d col = 0,6 m , Columns spacing S(c/c) = 1m

Poison ratio module ν = 0,2

Columns Height H = 20m

GWT = 0 ground water table on the soil surface

Columns undrained shear strength Cu col = 100 Kpa

$$E_{col} = 20 \,.\, c_{u,col}^{1.6} = 20 * (100)^{1,6} = 31.7\ Mpa$$

proportion column area per unit area:

$$\alpha = \frac{\pi d^2}{4s^2} = \frac{3{,}14\,.0{,}6^2}{4\,.1^2} = 0.283$$

From soil data $M_{soil} = 0{,}42\ Mpa$

From zone B: $M_{block} = \alpha . E_{col} + (1-\alpha) . M_{soil}$

$$M_{block} = 0{,}283\,.\,31{,}7 + (1-0{,}283).0{,}42 = 9{,}262\ Mpa$$

In our case $\eta_{LC} = 1$ as the columns extend to the firm bottom layer.

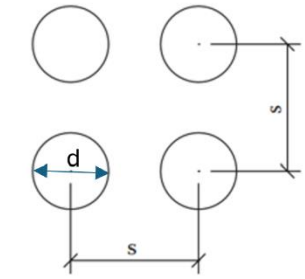

(a) Rectangular spacing

Figure 36 column area fraction modified from (Kirsch et al, 2012)

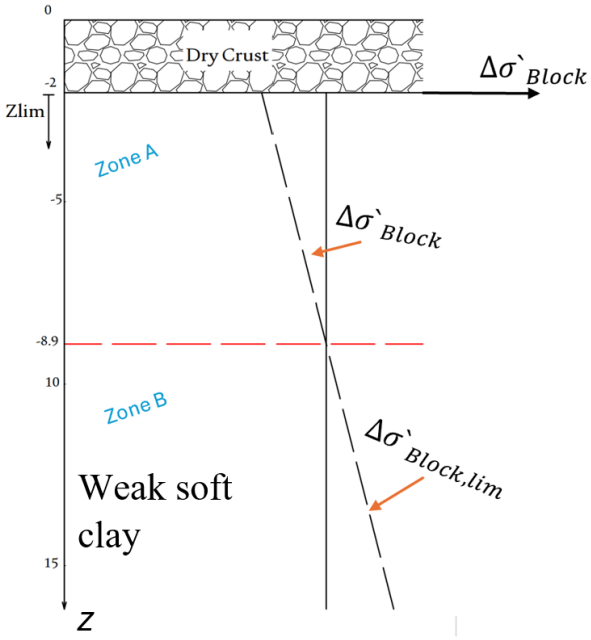

Figure 37 Plastic zone depth.

$$\Delta\sigma_{block,lim} = \frac{1{,}5\,.c_{u,col} + \sigma`_{v0}}{E_{col} - 1{,}5\,.M_{soil}}\,.M_{block}$$

$$= \frac{9{,}262\,.(1{,}5\,.100 + \left((17-10).2\right) + (14.2-10).z`)}{31{,}7 - 1{,}5\,.0{,}42} = q = 60\ \ldots\ldots Eq\ 11$$

By solving Equation (11) we got **z`= 8,9** m where z` starts from the top of clay layer under crust layer.

In plastic failure $\Delta\sigma`_{soil}(0) = \frac{2\,.q - 3\,.\alpha.c_{u,col}}{2+\alpha} = \frac{2\,.60 + 3\,.0{,}283\,.100}{2+0{,}283} = 15{,}42\ Kpa$

At the bottom of zone A $\Delta\sigma_{soil}(z_{lim}) = \frac{M_{soil}}{M_{block}}\,.\Delta\sigma_{block}\,(z_{lim})\ where\ \Delta\sigma_{block}\,(z_{lim}) = q = 60$

$$\Delta\sigma_{soil}(z_{lim}) = \frac{0{,}42}{9{,}262}\,.60 = 2{,}72\ Kpa$$

The avarage stress increase in zone A: $\Delta\sigma`_{soil} = \frac{\Delta\sigma`_{soil}(0) + \Delta\sigma`_{soil}(z_{lim})}{2} = \frac{15{,}42 + 2{,}72}{2} = 9{,}07\ Mpa$

The settlement in zone A: $\delta_A = \frac{\Delta\sigma`_{soil}}{M_{soil}}\,.z_{lim} = \frac{2{,}72\,.7{,}45}{0{,}42\,.1000} = 0{,}192m$

The settlement in zone B: $\delta_B = \frac{\Delta\sigma\text{block}\,.\text{zblock}}{\text{Mblock}} = \frac{(H - z`).q}{\text{Mblock}} = \frac{(20-9{,}45).60}{9{,}262\,.1000} = 0{,}06m$

The total settlement with columns $\delta = \delta_A + \delta_B = 0{,}161 + 0{,}068 = \mathbf{0,251m}$

Total settlement without columns $\delta = \frac{q}{M_{soil}}\,.H = \frac{60}{0{,}42\,.1000}\,.18 = \mathbf{2,571m}$

6-2- Application solved with Eurocode 7

$E_{col} = 31.7\ Mpa \quad q = 60KN/m^2 \quad D_{col} = 0{,}6m \quad c/c = 1m$

$H = 18m \quad \varphi`_c = 37^0 \quad \varphi`_s = 29.1^0 \quad K_0 = 0.52 \quad c`_{col} = 40\ KN/m^2$

$\sigma`_{v0} = 14 + 4.2h \quad and \quad c_{uk} = c`_{col}\,.\cos\varphi`_c + \sigma`_{v0}\,.\sin\varphi`_c$

$At \quad h = H/2 = 9m \rightarrow \sigma`_{v0} = 51.8\ Kpa \quad c_{uk} = 63.11\ KN/m^2$

$\sigma`_h = K_0.\sigma`_{v0} \quad and \quad \sigma`_{ult} = 2.c_{uk} + 3.\sigma`_{v0} \quad \leftrightarrow \quad \sigma`_h = 26.45\ Kpa\ , \quad \sigma`_{ult} = 205.59\ Kpa$

$q_{col} = 0.9.\ \Omega_c.\sigma`_{ult} \quad and \quad q_{soil} = q - q_{col} \quad \leftrightarrow \quad q_{col} = 52.36\frac{KN}{m^2}, \quad q_{soil} = 7.64\ KN/m^2$

The settlement then:

$$S_{col} = \sum\frac{q_{col}.\Delta h}{\Omega_c\,.E_{col}} \quad and \quad S_{soil} = \sum\frac{q_{soil}.\Delta h}{(1-\Omega_c)\,.M_{soil}} \quad ,the\ total\ settlement\ S = S_{col} + S_{soil}$$

$s_{col} = 0.105m \quad , \quad s_{soil} = 0.456m \quad and\ the\ total\ settlement\ is \quad \boldsymbol{S = 0.562m}$

6-3- Application solved with Plaxis

A half of the embankment were modelled with Plaxis software taking in account the ground water table at the ground surface, and the embankment, top dry crust layer, and the soft clay layer parameters. The boundary conditions were set to match soil geometry conditions. Figure (40) show the soil constitutive model of both unimproved and improved soil:

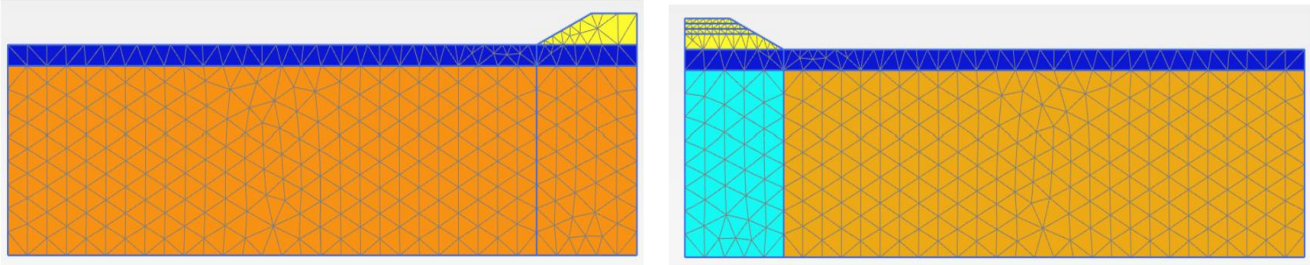

Figure 38 a) natural, (b) improved soil constitutive model.

The soil was modelled as VAT user defined S-CLAY1S soil model, in plaxis constitutive model, table 9-1 shows the soft clay parameters as S-CLAY1S model:

γ(KN/m³)	κ	ν`	λ	M	ω	ωd	ξ	ξ d	α_o	χ_o
14.2	0.165	0.17	1.367	1.17	0	0	0	0	0	0

Table 9-1 S-CLAY1S Soft clay parameters.

The columns were modelled as VAT user defined MNhard soil model directly under the embankment in plaxis constitutive model, table 9-2 shows the columns parameters as MNhard model for columns diameter 0.6m and columns spacing:

γ(KN/m³)	G_{ur}^{ref} (KN /m²)	ν`	c`	φ`	ψ	m	P_{ref}	R_f	G_{50}^{ref} (KN /m²)	Ω
14.2	12000	0.35	40	37	0	0.7	100	0.9	4000	0.283

Table 9-2 MNhard column parameters

Where Ω= 0.283 for column diameter of D=0.6m and for column spacing c/c=1m.

The embankment soil was modelled as drained Mohr-Columb soil model. The top dry crust layer was modelled as drained Mohr-Columb soil model. Plaxis stages were divided to cover several time stages starting from the construction period leading to the initial consolidation stage of the soil after one hundred years of time.

7- Results

The results include first the results of one column diameter D = 0.6m and one column spacing c/c = 1m, as mentioned above in chapters 6-1 to 6-3, later the results were calculated for another diameter of 0.8m of columns and for many spacings for each diameter. The results were calculated with deep mixing Swedish method, with Eurocode 7 method, and with volume averaging techniques VAT in plaxis method. Plaxis results were only calculated for isotropic soft soil. The results of column diameter D = 0.6m and one column spacing c/c = 1m are shown in the table

Method	Total settlement (m) before improvement	Total settlement (m) After improvement
Swedish method	2.57	0.25
Swedish settlement calculation	1.89	
Classic international method	1.47	
Eurocode 7		0.56
Plaxis	1.45	0.32

Table 10 settlement results for D=0.6m and c/c=1m

Table (10) shows the results according to various settlement calculation methods, where the final settlement is the lonely value to be considered in hand numeric calculations. Plaxis software can give

different outputs of results according to its large analysis capacity. The hand calculations were done by Excel to extract the soil parameters from the soil raw data and to calculate the results for many column diameters and spacings. Figure (39) shows the results of settlements for one diameter of 0.6m, and one spacing of 1m for columns for both improved and unstabilased natural soil. Where the results were calculated by different settlement calculation methods as shown in this figure.

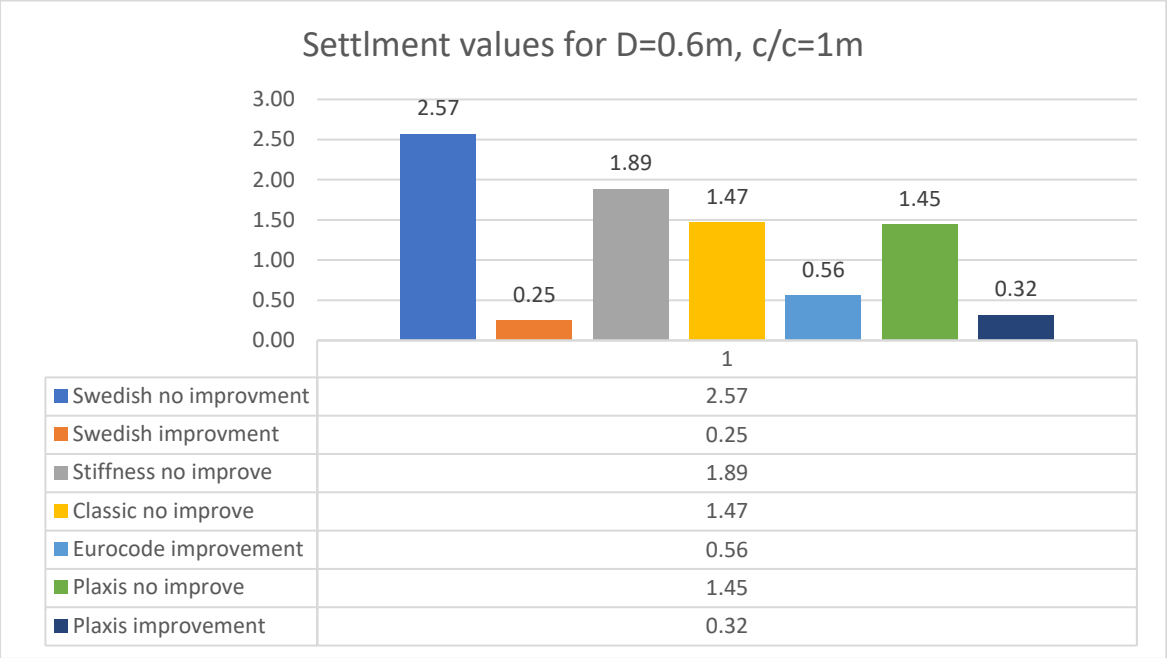

Figure 39 Settlement values for one diameter and one spacing of column.

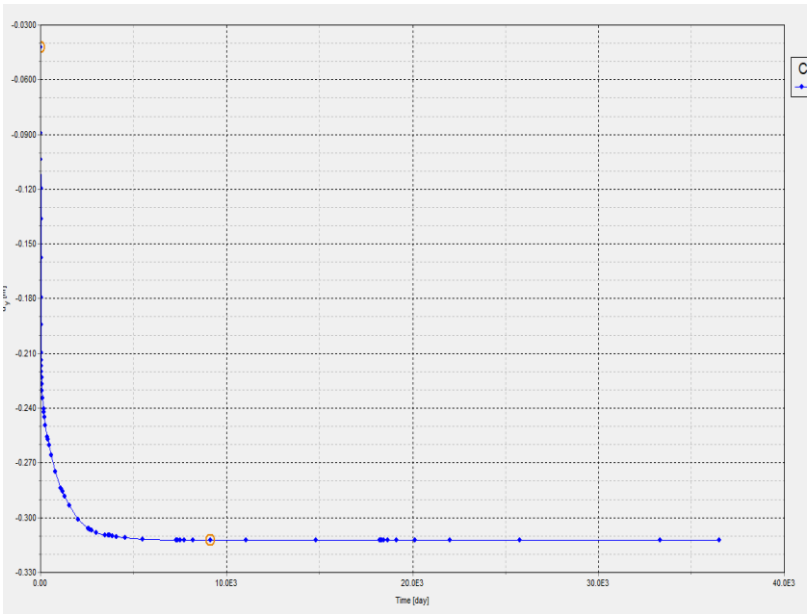

Figure 40 Plaxis vertical settlement uy for D=0.6, c/c=1m

Later on the settlement calculations were performed for several spacings and for tow diameters. The results were calculated according to: Swedish method, Eurocode 7 as presented in (Vogler 2008), and with volume averaging techniques using finite element modelling in Plaxis. Table (11) shows the result values of settlement for tow columns diameter D=0,6m and D=0.8m, and for several spacings 0.8m, 1.0m, 1.2m, and 1.4m. for Swedish method Z_{lim} values were presented in the results to clarify the depth of plastic zone in Swedish method results and to compare it with the total height of the soft clay layer

which is H = 18m, for many spacings the resulted plastic zone was higher than clay layer height. Z_{lim} values start from the soft clay level under the dry crust layer at a level of -2m from ground surface, see figure (37). The results varied according to the variation of columns diameter and spacings, and according to the calculating method. The settlement always increased wherever the volume fraction was smaller. Bigger diameter with smaller spacing gave the bigger volume fraction of columns and the less settlement. As shown in table (11).

Diametre (m)	0.6					0.8			
Spacing c/c (m)	0.8	1.0	1.2	1.4		0.8	1.0	1.2	1.4
Volume fraction Ω	0.442	0.283	0.196	0.144		0.785	0.502	0.349	0.256
Z_{lim} (m)	0.00	8.88	28.7*	51.0*		0.00	0.00	0.11	13.6
$\delta_{Swedish}$	0.084	0.251	0.666	0.836		0.043	0.076	0.096	0.389
			1.08*	2.48*					
δ_{plaxis}	0.224	0.324	0.476	0.653		0.142	0.204	0.269	0.358
$S_{Eurocode}$	0.077	o.562	1.370	1.775		0.043	0.068	0.089	0.833

**The value was calculated according to the out-of-range Z_{lim} value.*

Table 11 settlement results for many diameters and many spacing.

Figures (41 & 42) show the settlement results for column diameters of 0.6m and 0.8m calculated exclusively from plaxis software.

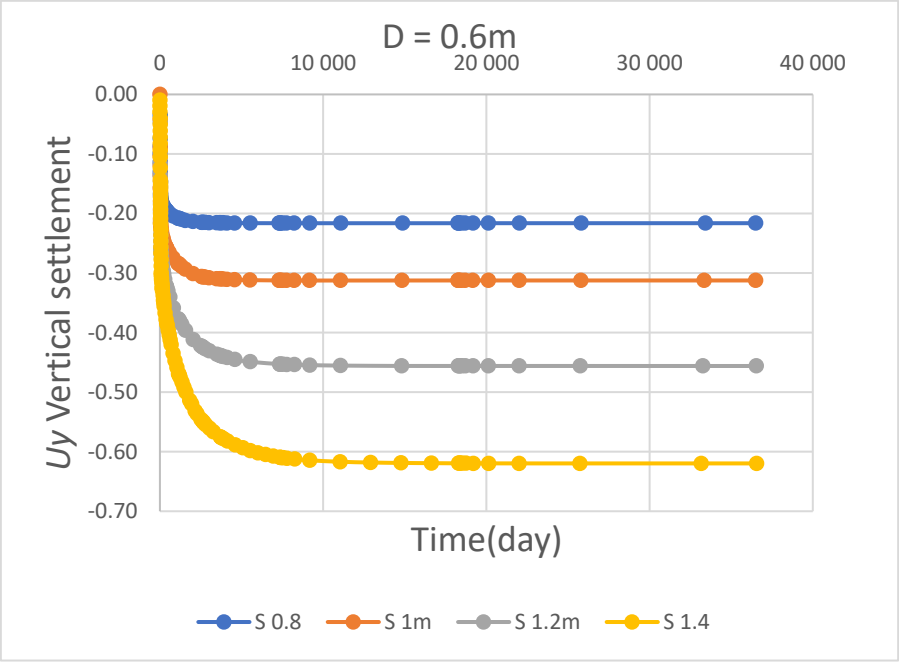

Figure 41 Plaxis vertical settlement results for diameter D=0.6m

The results are for vertical settlements only and they were presented for isotropic conditions. Plaxis results also show that for each column diameter the vertical settlement u_y were increased by increasing the spacings between columns. For vertical displacements the maximum vertical displacement is estimated under the centre of the embankment, while for horizontal displacements *ux* the maximum value located at the cross point of the end of embankment toe with the soft soil see fig (44) at point A or around it. The maximum horizontal displacement from Plaxis analysis results for unstabilised soil is about 0.33m, this equals about 20% from the vertical displacement, besides the Swedish method does not calculate it, though it is excluded from the results discussion.

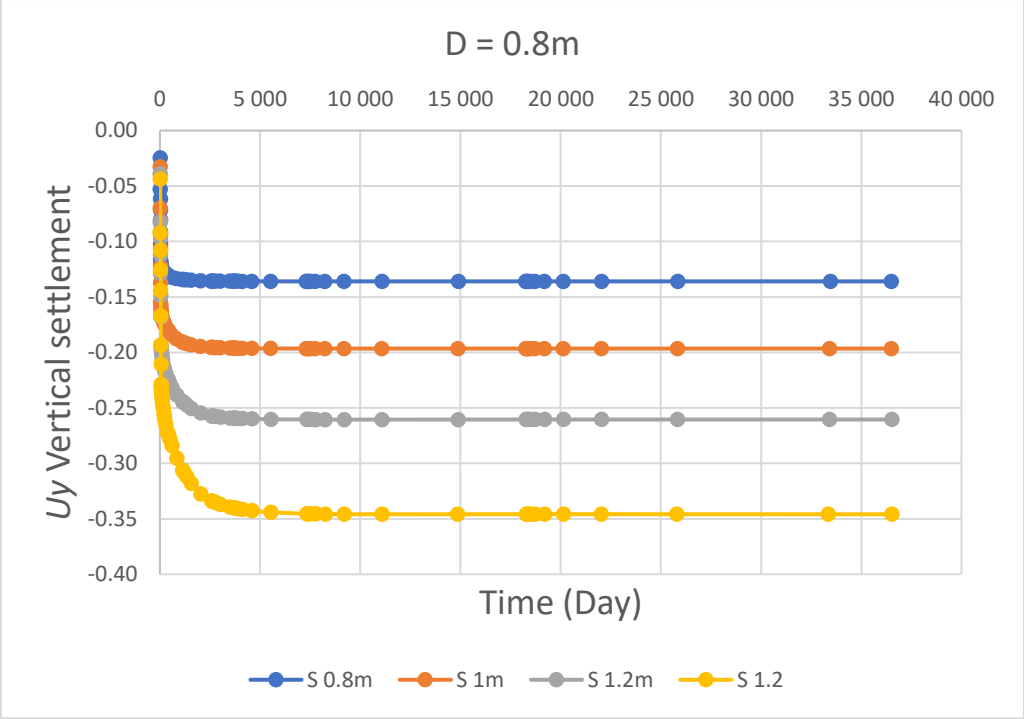

Figure 42 Plaxis vertical settlement results for diameter D=0.8m

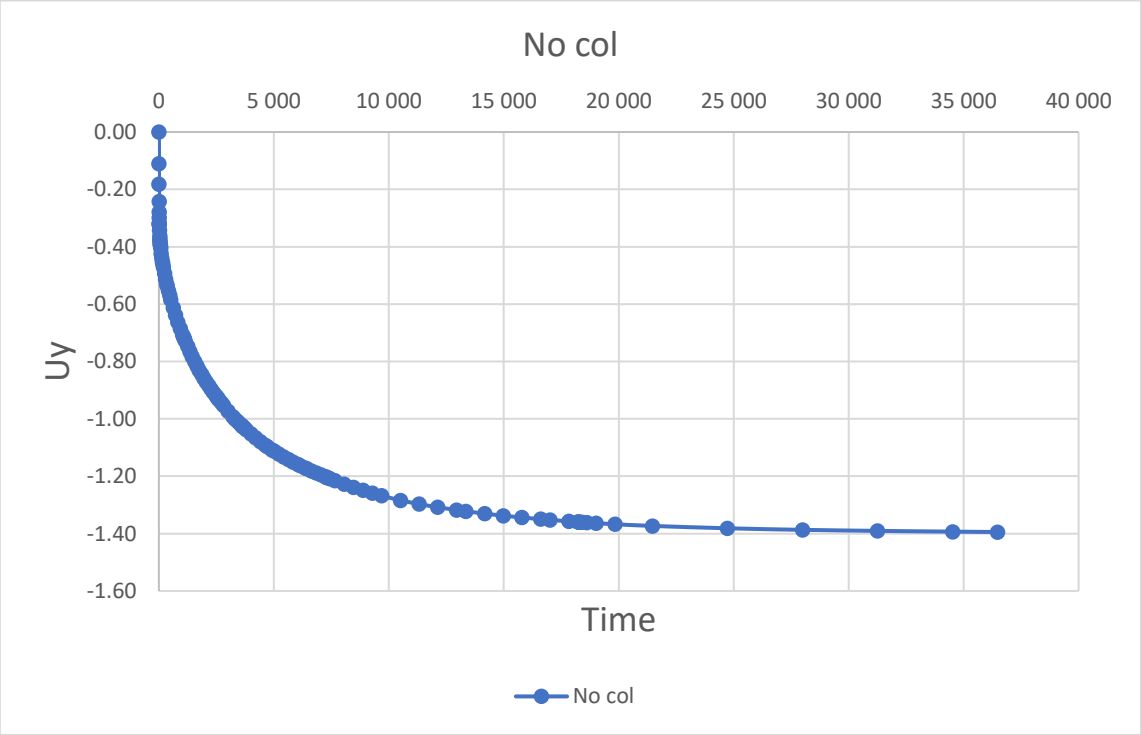

Figure 43 Plaxis vertical Settlement for unstabilized soil.

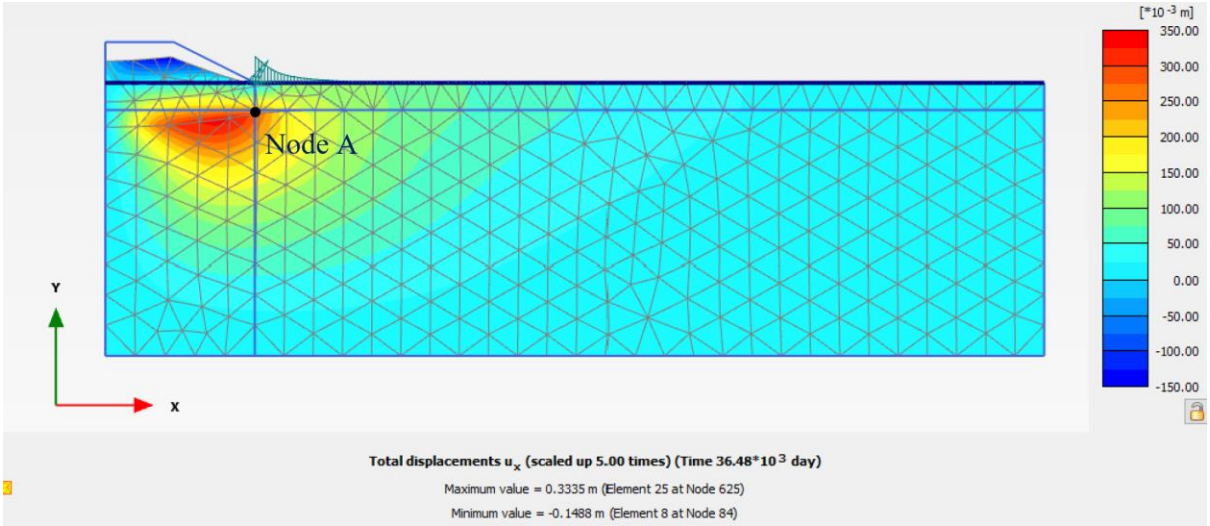

Figure 44 maximum horizontal deformation for unstabilized soil.

Figures (45, 46, and 47) show the variation of settlements for each column diameter according to the variation of spacing between columns for Swedish method results, for Plaxis results, and for both of them combined in one chart, in figure (47).

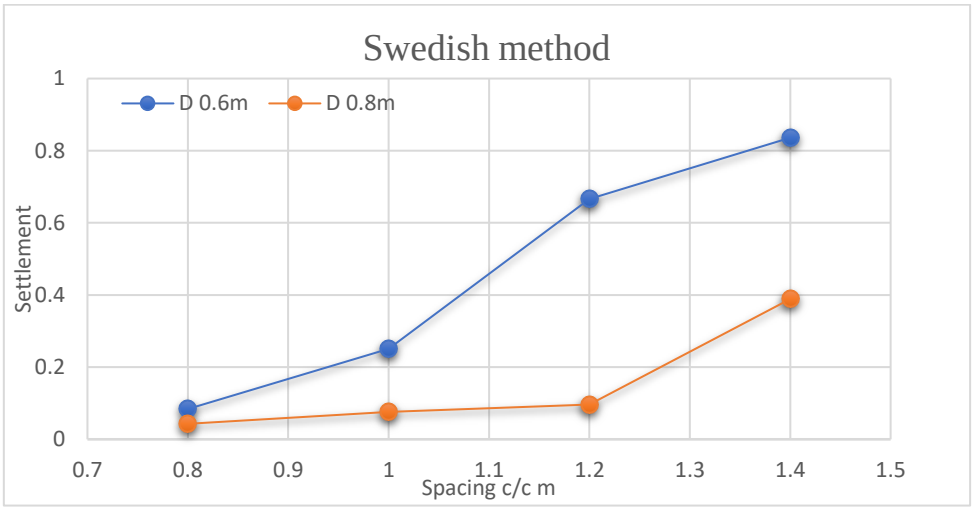

Figure 45 Settlement variation according to the spacing variation in Swedish method.

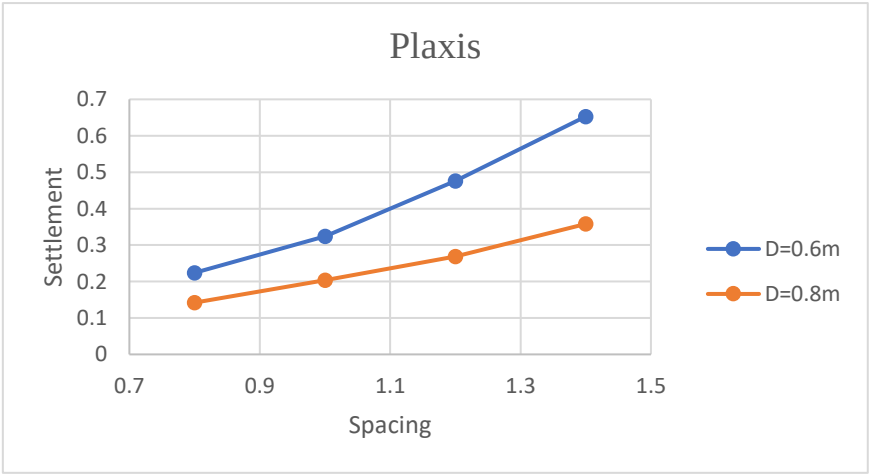

Figure 46 Settlement variation according to the spacing variation in Plaxis method.

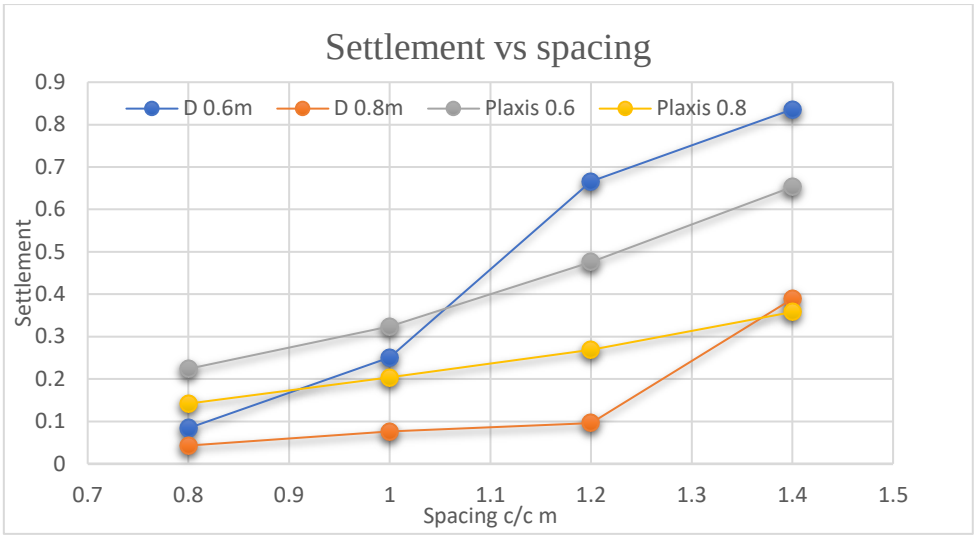

Figure 47 Settlement variation according to the spacing variation in both Swedish method and Plaxis method.

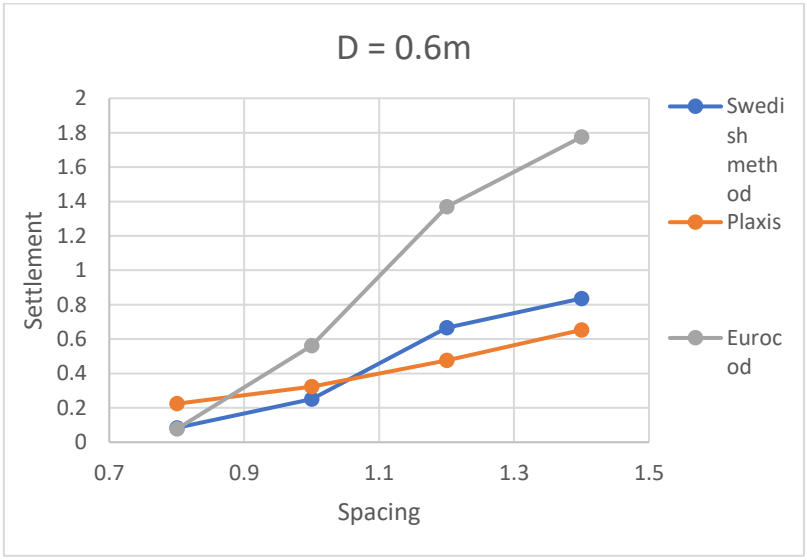

Figure 48 Settlemnt variation according to the spacing variation for Swedish method, Eurocode, and Plaxis ***D=0.6m.***

**The settlement for out-of-range Z_{lim} values were not included in these above and below charts*

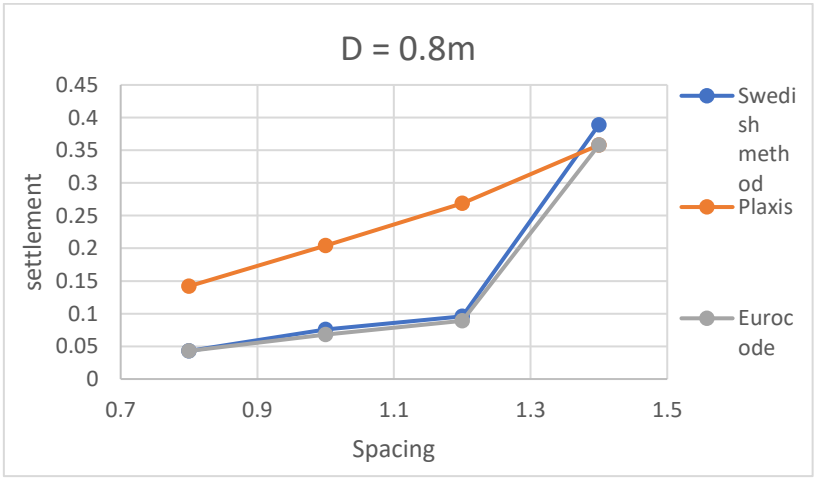

Figure 49 Settlement variation according to the spacing variation for Swedish method, Eurocode, and Plaxis ***D=0.8m.***

8- Discussion

Based on the presented results for diameter 0.6m of columns and spacing of 1m as shown in table (10) and figure (41). The total displacement of unstabilised soil was 2.571 m when calculated with Swedish method and it was 1.45 m when calculated with Plaxis software. In the contrary the total displacement of improved soil was 0.25 m when calculated with Swedish method and 0.32 m when calculated with Plaxis. Even when the initial settlement was calculated for unstabilised soil with other calculation methods the results were lesser than the value calculated by Swedish method as shown in table (10) and figure (39). The details of settlement calculations for the other methods are detailed in the Appendix of this thesis, see tables (14 & 15). This discrepancy in results could be because of the very simplicity in the behaviour of the modelling in Swedish method if compared with the other calculation methods especially if compared with the nonlinear analysis of Plaxis finite element constitutive modelling. Swedish method results were closer to Plaxis results for D=0.6m diameter of column, figures (47, 48), and the results were more divergent for 0.8m diameter of columns, figure (49). Plaxis results were somehow parallel for the tow chosen diameter of columns when the spacing changed fig (46). The results were more divergent for Swedish method results figure (45). For column diameter of 0.8m the euro code results were closer to the results calculated by Swedish method figure (49) if compared with plaxis results, the results were very much close for spacing of 1.4m and a diameter of 0.8m of column for plaxis, Swedish method, and Eurocode. For column diameter of 0.6 the Swedish method results were closer to plaxis results when the spacing changed, figure (48), if compared with column diameter of 0.8m figure (49). There is no available laboratory tests or in-situ observations to compare the theoretical and the calculated results with, and this is a main essential limitation of this thesis.

Swedish method is a simple method to calculate the predicted initial settlement of unstabilised soil and the estimated settlement of improved soil. Although its values for unstabilised soil were higher than many of another settlement calculation methods especially plaxis results. In the contrary, its estimated settlement values for improved soil were lower than another settlement calculation methods especially plaxis and Eurocode 7 methods. The estimated linear behaviour of soft clay in zone B simplifis the problem and the mathematical solution of it, whereas this linear behaviour is mostly unrealistic for soft soils as clay, especially when the soil pore pressure varies due to soil water conditions and soil loading forces from the above located embankment. Plus, the estimation of horizontally layered soil is not always valid in situ conditions. A multi soft soil layers can make the calculations of settlement for Swedish method more difficult due to the defining of the depth of plastic zone Z_{lim} and in which layer it goes through. The variation of stiffness between soft soil and hard columns has its impact, figure (25) as the columns acts as stiff material while the soft soil acts as ductile plastic material. The column with small diameter can fails at a relatively small lateral strain if compared with plastic soil deformations. Swedish method calculates only the vertical settlement and does not refer to the horizontal deformations due to the embankment loading especially at the basement of embankment toe. The permeability of columns has no effect on the results for Swedish method, whereases, the permeability of improved soil varies depending on the type and the amount of stabilised binders and the mixing method.

Finite element Plaxis simulation can predict the non-linear behaviour of soil especially if good and valid parameters were used in the inputs of the Plaxis constitutive modelling, the gained results can display wide range of soil behaviour outputs, starting from detailed vertical, horizontal, and total deformations to the detailed stresses and the impact of boundary conditions, and the pore pressure changes during every inputted stage of the analysis. These complete amounts of outputs can guide the designer and the contractor within the designing and the construction processes and help the prediction of risks during the project life cycle. The estimation of perfect interaction between soil a columns material has its impact on the results for both Swedish and Plaxis analysis especially in case of creep. Plaxis can handle with creep cases while Swedish method has no estimations for creep cases. Plaxis constitutive modelling included S-CLAY1S and MNhard soil modelling with isotropic soil conditions. Paxis results

showed the non-linear behaviour of unstabilised soil and improved columns due to loading and pore pressure change within the consolidation of the soil blocks. Horizontal deformation of the soil showed in Plaxis where the maximum value is located around the toe of embankment at point A, see figure (44). The maximum value equals approximately about 20% of the maximum vertical settlement of unstabilised soil, and it was neglected due to its small value in this case. Based on presented results there is a typical value of column diameter and column spacing that results the best volume fraction of columns Ωc, which generates the desired initial or time dependent settlements. Plaxis analysis can correctly predict the stresses, strains, and settlements values at any given stage during the project life cycle, while these predictions are very limited or dose not exist in Swedish method calculations.

The estimation of horizontally layered soil, and the simple estimated linear behaviour of zone B block in Swedish method can affect the actual results that may noticed if a real field measurement were done.

9- outlook and future work

As the anisotropic analysis could produce different settlement results, a further future anisotropy analysis is recommended to this case study for correctly discuss and judge the results and the differences between finite element analysing methods and hand calculating methods. Based on the above presented results and on engineering background, the computational finite element analysing methods were always relevant methods for predicting realistic results especially when the correct and valid inputs were interred to the computational analysis modelling. Finite element methods depend heavily on the right, correct, and valid inputs that must be tested, experimented, and deprived, to correctly calculate and present right and valid outputs and results.

The final economic and practical method to improve the soils and reshape them to sustain the constructions on/or within it depends on the available resources and the economical and far-sighted engineering situation of the project. Engineers are responsible to innovate, calculate, analyse and create the best and economic engineering solutions of the problems, this is the burden that they should be proud to bear and take responsibility of.

References:

- Andrew Lees 2016 Geotechnical Finite Element Analysis, n.d.
- Åhnberg, H., Lunds tekniska högskola. Institutionen för byggnadsteknik., KFS), 2006. Strength of stabilised soils : a laboratory study on clays and organic soils stabilised with different types of binder. Department of Construction Sciences, Lund University.

Alén, C., Baker, S., Bengtsson, P.-E., Sällfors, G., 2005a. Lime/Cement column stabilised soil-A new model for settlement calculation, in: Deep Mixing'05.

Alén, C., Baker, S., Bengtsson, P.-E., Sällfors, G., 2005b. Lime/cement column stabilised soil-a new model for settlement calculation, in: Deep Mixing'05.

Becker, P., Karstunen, M., 2013. Volume Averaging Technique in numerical modelling of floating deep mixed columns in soft soils. CRC Press Boca Raton, FL, USA.

Benz, T., 2007. Small-strain stiffness of soils and its numerical consequences. Univ. Stuttgart, Inst. f. Geotechnik Stuttgart.

Brinkgreve, R.B.J., Vermeer, P.A., 2002. Plaxis finite element code for soil and rock analyses, Version 8. Balkema Rotterdam.

EN 14679, 2005, 2006. Execution of special geotechnical works : deep mixing. BSI.

EuroSoilStab, 2002. Development of design and construction methods to stabilise soft organic soils. Design guide soft soil stabilisation.

Geotechnical Finite Element Analysis, n.d.

Horpibulsuk, S., Miura, N., Nagaraj, T.S., 2003. Assessment of strength development in cement-admixed high water content clays with Abrams' law as a basis. Geotechnique 53, 439–444.

Hossain, S., Rao, K.N., 2006. Performance evaluation and numerical modeling of embankment over soft clayey soil improved with chemico-pile. Transp. Res. Rec. 1952, 80–89.

Karstunen, M., Krenn, H., Wheeler, S.J., Koskinen, M., Zentar, R., 2005. Effect of anisotropy and destructuration on the behavior of Murro test embankment. Int. J. Geomech. 5, 87–97.

Karstunen, M., Wiltafsky, C., Krenn, H., Scharinger, F., Schweiger, H.F., 2006. Modelling the behaviour of an embankment on soft clay with different constitutive models. Int. J. Numer. Anal. Methods Geomech. 30, 953–982.

Kempfert, H.-G., 2006. Excavations and foundations in soft soils. Springer.

Kirsch, K., Bell, A., 2012. Ground improvement. CRC Press.

Koskinen, M., Karstunen, M., Wheeler, S.J., 2002. Modelling destructuration and anisotropy of a soft natural clay.

Larsson, R., 2006. Djupstabilisering med bindemedelsstabiliserade pelare och masstabilisering-En vägledning. Sven. Djupstabilisering SD Rapp. 17.

Larsson, S., 2021. The Nordic dry deep mixing method: Best practice and lessons learned, in: Deep Mixing-An Online Conference. DFI Deep Foundation Institute, p. 30 p.

Leoni, M., 2009. Geotechnics of Soft Soils: Focus on Ground Improvement. CRC Press/Balkema.

Matsuoka, H., Nakai, T., 1982. A new failure criterion for soils in three-dimensional stresses.

Nagaraj, T.S., Yaligar, P.P., Miura, N., Yamadera, A., 1998. Predicting strength development by cement admixture based on water content. Geotech. Eng. Bull. 7.

Toll, D.G., Abedin, Z., Buma, J., Cui, Y., Osman, A.S., Phoon, K.K., 2012. The impact of changes in the water table and soil moisture on structural stability of buildings and foundation systems: systematic review CEE10-005 (SR90).

Topolnicki, M., 2003. Ground improvement with in-situ wet soil mixing.

Vogler 2008, n.d. Numerical Modelling of Deep Mixing with Volume Averaging Technique.

Von Soos, P., 1990. Properties of soil and rock (in German), Grundbau Taschenbuch part 4. Ernst Sohn Berl. 1–10.

Wheeler, S.J., Näätänen, A., Karstunen, M., Lojander, M., 2003. An anisotropic elastoplastic model for soft clays. Can. Geotech. J. 40, 403–418.

X-Appendix

A-Soil stiffness and compression modulus calculated from estimated soil sample data as shown in tables (12 & 13) and figure (51).

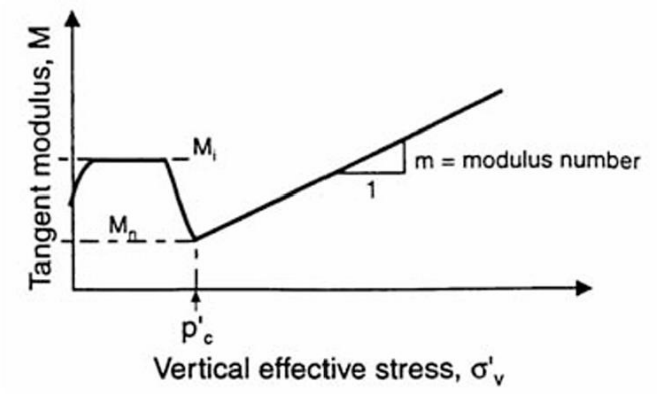

Figure 50 compression modulus (Vogler, 2008)

SAMPLE 12		Vo
4.13 - 4.22 m		3.024
Stress (kPa	Void ratio	strain%
6.75	3.011	0.996
13.5	2.990	0.989
27	2.945	0.974
54	2.686	0.888
108	2.050	0.678
162	1.819	0.602
216	1.684	0.557
324	1.524	0.504
27	1.656	0.548

SAMPLE 13		Vo
4.34 - 4.37 m		3.034
Stress (kPa	Void ratio	strain%
6.75	3.015	0.994
13.5	2.998	0.988
27	2.961	0.976
54	2.886	0.951
108	1.938	0.639
162	1.723	0.568
216	1.644	0.542
324	1.425	0.470
27	1.605	0.529
54	1.581	0.521
108	1.528	0.504
216	1.457	0.480
324	1.380	0.455
6.75	1.611	0.531

SAMPLE 14		Vo
5.20 - 5.23 m		2.922
Stress (kPa	Void ratio	strain%
6.875	2.920	0.999
13.75	2.891	0.989
27.5	2.859	0.979
55	2.810	0.962
110	1.985	0.679
165	1.761	0.603
220	1.677	0.574
440	1.359	0.465
27.5	1.561	0.534
55	1.541	0.528
110	1.479	0.506
220	1.414	0.484
13.75	1.585	0.542

SAMPLE 15		Vo
6.06 - 6.12 m		2.371
Stress (kPa	Void ratio	strain%
10	2.344	0.989
20	2.325	0.981
40	2.293	0.967
60	2.266	0.956
80	2.223	0.937
100	2.098	0.885
150	1.828	0.771
200	1.660	0.700
300	1.425	0.601
400	1.370	0.578
800	1.112	0.469
25	1.314	0.554
50	1.311	0.553
100	1.275	0.538
200	1.220	0.514
25	1.289	0.544

Table 12 soil oedometer test samples

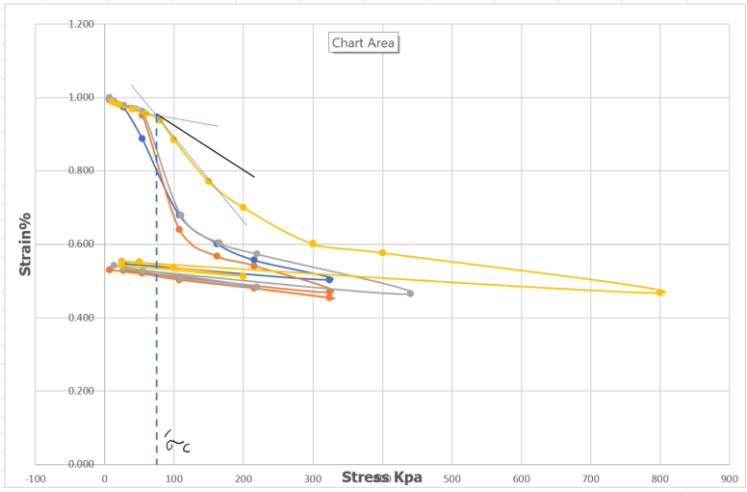

Figure 51 Soil stiffness and pre-consolidation parameters.

sample	12	13	14	15	avarage
M0	0.92	1.10	1.30	1.35	1.17
ML	0.38	0.28	0.30	0.70	0.42
σ´c	41.45	51.95	54.1	80	56.88

Table 13 Swedish method soil parameters.

B-Settlement calculations according to the Swedish settlement calculations method.

slice	γsoil	Z	σz	U	σ´z	Δσ´z	σ´z+Δσ´z	δc
		0	0.00	0.00	0.00	60.00	60.00	0
	17	2	34.00	20.00	14.00	55.00	69.00	0
1	14.2	3	48.20	30.00	18.20	53.36	71.56	0.135963
2	14.2	5	76.60	50.00	26.60	49.41	76.01	0.142783
3	14.2	7	105.00	70.00	35.00	46.00	81.00	0.152198
4	14.2	9	133.40	90.00	43.40	43.03	86.43	0.163707
5	14.2	11	161.80	110.00	51.80	40.42	92.22	0.176929
6	14.2	13	190.20	130.00	60.20	38.11	98.31	0.19157
7	14.2	15	218.60	150.00	68.60	36.05	104.65	0.2074
8	14.2	17	247.00	170.00	77.00	34.21	111.21	0.224237
9	14.2	19	275.40	190.00	85.40	32.54	117.94	0.241932
10	14.2	20	289.60	200.00	89.60	31.76	121.36	0.251064
								1.887783

Table 14 Settlement calculations according to the Swedish settlement method

C-Settlement calculations according to the international consolidation calculation method.

slice	σ`p	γsoil	Z	σz	U	σ´z	Δσ´z	σ´z+Δσ´z	δc
	0		0	0.00	0.00	0.00	60.00	60.00	0.000
	0	17	2	34.00	20.00	14.00	55.00	69.00	0.000
1	41.45	14.2	2.5	41.10	25.00	16.10	53.88	69.98	0.334
2	41.45	14.2	4	62.40	40.00	22.40	50.77	73.17	0.269
3	41.45	14.2	6	90.80	60.00	30.80	47.14	77.94	0.211
4	41.45	14.2	8	119.20	80.00	39.20	44.00	83.20	0.171
5	41.45	14.2	10	147.60	100.00	47.60	41.25	88.85	0.207
6	41.45	14.2	12	176.00	120.00	56.00	38.82	94.82	0.233
7	56.8	14.2	14	204.40	140.00	64.40	36.67	101.07	0.016
8	56.8	14.2	16	232.80	160.00	72.80	34.74	107.54	0.013
9	56.8	14.2	18	261.20	180.00	81.20	33.00	114.20	0.011
10	56.8	14.2	19	275.40	190.00	85.40	32.20	117.60	0.005
									1.471732

Table 15 Settlement according to the international consolidation method.

D-POP: Table (16) and figure (53) show how POP value calculated.

Depth	Total sigma	U	Sigma'	Sigma c'
0	0	0	0	
1	17	0	17	
2	34	10	24	
2.325	38.485	13.25	25.235	51.47
3	47.8	20	27.8	
3.06	48.628	20.6	28.028	49.91
3.105	49.249	21.05	28.199	
3.217	50.7946	22.17	28.6246	52.51
3.235	51.043	22.35	28.693	46.77
3.5	54.7	25	29.7	
4	61.8	30	31.8	
4.175	64.285	31.75	32.535	41.45
4.355	66.841	33.55	33.291	51.95
5	76	40	36	
5.215	79.053	42.15	36.903	54.1
6	90.2	50	40.2	
6.09	91.55	50.9	40.65	
6.135	92.225	51.35	40.875	
6.175	92.825	51.75	41.075	
6.355	95.525	53.55	41.975	48.2
10	150.2	90	60.2	
15	225.2	140	85.2	
15	225.2	140	85.2	
20	305.2	190	115.2	

Table 16 effective stress with depth

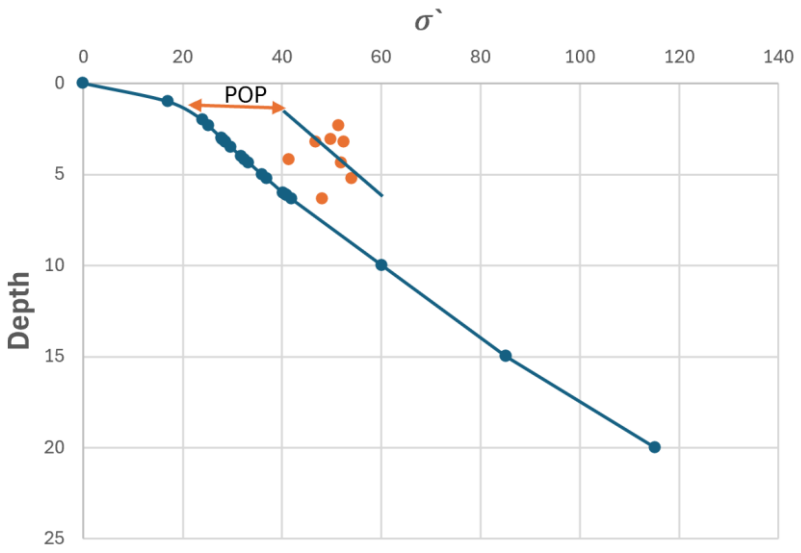

Figure 52 POP values

E-*Cc* and *Cs* values: Table (17 & 18) and figure (54) show *Cc* and *Cs* calculations. Cc and Cs values were calculated and extracted from soil data and with Python programming code.

SAMPLE 12		SAMPLE 13		SAMPLE 14	
4.13 - 4.22 m		4.34 - 4.37 m		5.20 - 5.23 m	
Stress (kPa)	Void ratio	Stress (kPa)	Void ratio	Stress (kPa)	Void ratio
6.75	3.011	6.75	3.015	6.875	2.920
13.5	2.990	13.5	2.998	13.75	2.891
27	2.945	27	2.961	27.5	2.859
54	2.686	54	2.886	55	2.810
108	2.050	108	1.938	110	1.985
162	1.819	162	1.723	165	1.761
216	1.684	216	1.644	220	1.677
324	1.524	324	1.425	440	1.359
27	1.656	27	1.605	27.5	1.561
		54	1.581	55	1.541
		108	1.528	110	1.479
		216	1.457	220	1.414
		324	1.380	13.75	1.585
		6.75	1.611		

Table 17 Cc and Cs values

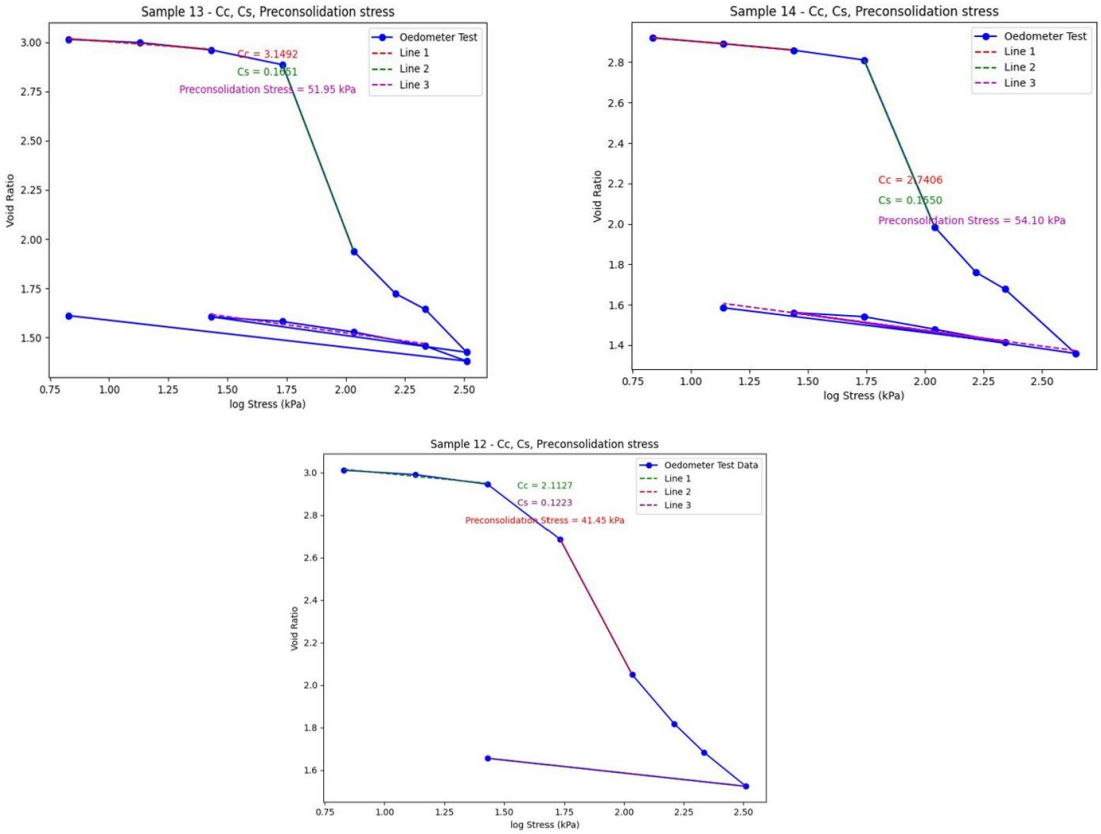

Figure 53 Cc and Cs values.

sample	12	13	14	
σ´c	41.45	51.95	54.1	Kpa
Cc	2.1127	3.1492	2.7406	
Cs	0.1223	0.1651	0.155	

Table 18 soil parameters from soil data.

F-Stress ratio-shear strain ratio to deprive critical state *Mc* value. Table (19) and figure (54) show how *Mc* were deprived.

Shear strain	Stress ratio
0.00645929	0.444803
0.193116	0.698471
0.64506	1.02043
0.828694	1.06595
1.01266	1.13429
1.21385	0.98876
1.21079	0.777764
1.18901	0.677979
1.15009	0.797756
1.37757	1.06281
1.56149	1.12829
1.70418	1.15388
1.96913	1.19935
3.12783	1.19018
3.39237	1.20715
3.6767	1.18704
4.36793	1.18667
4.57132	1.19226
4.81503	1.17502
5.0592	1.18915
6.38091	1.20555
7.74333	1.22478
8.69905	1.23853
9.26838	1.24392
9.79697	1.24364
9.79407	1.04405
9.66828	0.781796
9.46071	0.488221
9.19335	0.277366
9.0286	0.132037
8.94604	0.0465411
8.86712	0.21196
8.86877	0.326012
8.84902	0.365941
8.95138	0.414359
9.17973	0.739288

9.50916	1.02424
9.7144	1.15815
10.3452	1.19488
11.1794	1.2429
11.6472	1.25406
11.5633	1.08017
11.4175	0.835036
11.3123	0.59273
11.1674	0.413174
11.0226	0.242172
10.9607	0.179476

Table 19 Stress ratio-strain ratio.

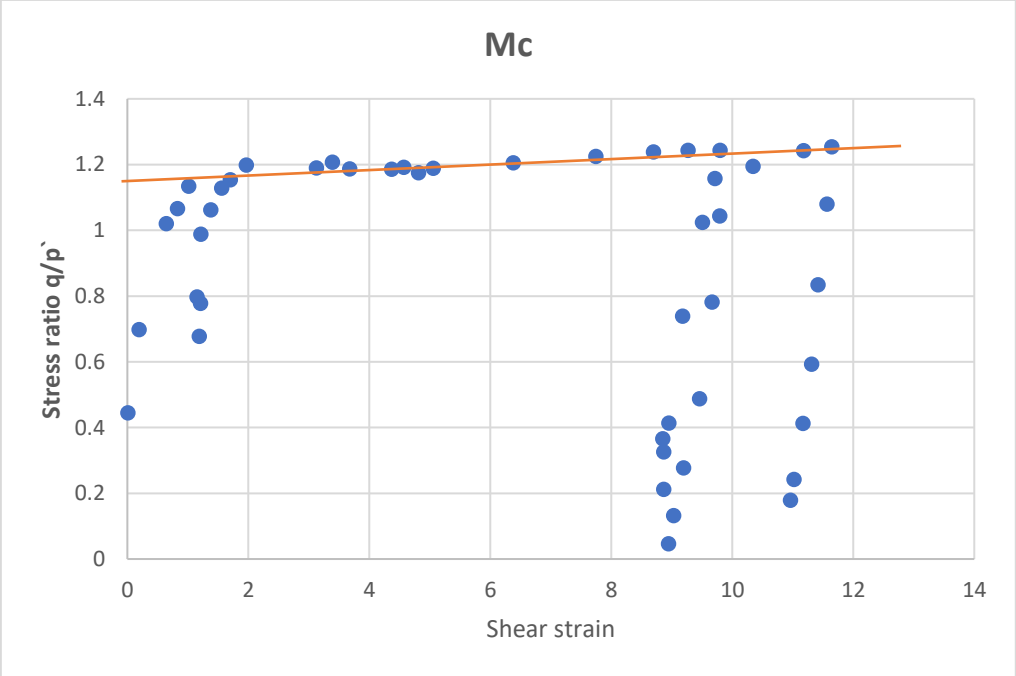

Figure 54 stress ratio-strain ratio from triaxial test data.

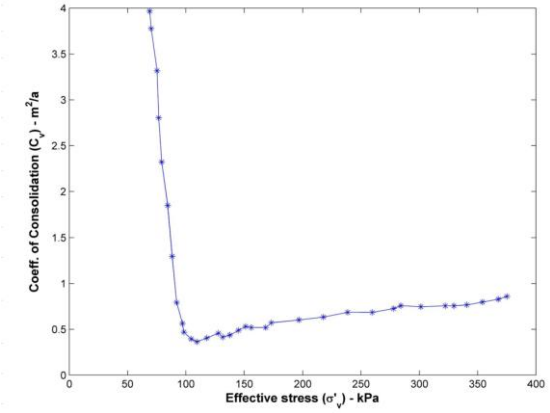

Figure 55 Coefficient of compression Cv values for depth 5 m.